Measurement of the rapidity and transverse momentum distributions of Z Bosons in pp Collisions at $\sqrt{s} = 7TeV$

CMS Collaboration ; Amsler, C ; Chiochia, V ; Chatrchyan, S ; Khachatryan, V ; Sirunyan, A M ; Tumasyan, A ; Aguiló, E ; De Visscher, S ; Favaro, C ; Ivova Rikova, M ; Millan Mejias, B ; Otiougova, P ; Robmann, P ; Schmidt, A ; Snoek, H ; Verzetti, M ; et al

Abstract: Measurements of the normalized rapidity (y) and transverse-momentum (qT) distributions of Drell–Yan muon and electron pairs in the Z-boson mass region (60<M <120 GeV) are reported. The results are obtained using a data sample of proton-proton collisions at a center-of-mass energy of 7 TeV, collected by the CMS experiment at the Large Hadron Collider (LHC), corresponding to an integrated luminosity of 36 pb-1. The distributions are measured over the ranges |y|<3.5 and qT<600 GeV and compared with quantum chromodynamics (QCD) calculations using recent parton distribution functions to model the momenta of the quarks and gluons in the protons. Overall agreement is observed between the models and data for the rapidity distribution, while no single model describes the Z transverse-momentum distribution over the full range.

DOI: https://doi.org/10.1103/PhysRevD.85.032002

EUROPEAN ORGANIZATION FOR NUCLEAR RESEARCH (CERN)

CERN-PH-EP/2011-169
2011/10/25

CMS-EWK-10-010

Measurement of the Rapidity and Transverse Momentum Distributions of Z Bosons in pp Collisions at $\sqrt{s} = 7$ TeV

The CMS Collaboration*

Abstract

Measurements of the normalized rapidity (y) and transverse momentum (q_T) distributions of Drell–Yan muon and electron pairs in the Z-boson mass region ($60 < M_{\ell\ell} < 120\,\text{GeV}$) are reported. The results are obtained using a data sample of proton-proton collisions at a center-of-mass energy of 7 TeV, collected by the CMS experiment at the LHC, corresponding to an integrated luminosity of 36 pb^{-1}. The distributions are measured over the ranges $|y| < 3.5$ and $q_T < 600\,\text{GeV}$ and compared with QCD calculations using recent parton distribution functions. Overall agreement is observed between the models and data for the rapidity distribution, while no single model describes the Z transverse-momentum distribution over the full range.

Submitted to Physical Review D

*See Appendix A for the list of collaboration members

1 Introduction

The production of Z and W bosons, which may be identified through their leptonic decays, is theoretically well described within the framework of the standard model. Total and differential cross sections have been calculated to next-to-next-to-leading-order (NNLO) [1, 2]. The dominant uncertainties in the calculation arise from imperfect knowledge of the parton distribution functions (PDFs), from the uncertainty in the strong-interaction coupling α_s, and from the choice of quantum chromodynamics (QCD) renormalization and factorization scales. Measurements of the inclusive Z and W production cross sections performed by the Compact Muon Solenoid (CMS) experiment [3] show agreement with the latest theoretical predictions both for the absolute value and for the ratios $\mathrm{W}^+/\mathrm{W}^-$ and W/Z. Likewise, agreement is found for the measurement of the dilepton mass distribution over a wide range [4].

In this paper, we present measurements of the normalized rapidity and transverse momentum distributions for Drell–Yan muon and electron pairs in the Z-boson mass region ($60 < M_{\ell\ell} < 120\,\mathrm{GeV}$). The results are obtained from a sample of proton-proton collisions at a center-of-mass energy of 7 TeV, recorded by the CMS detector at the Large Hadron Collider (LHC) in 2010, and corresponding to an integrated luminosity of $35.9 \pm 1.4\,\mathrm{pb}^{-1}$. The measurement of the rapidity (y) and transverse momentum (q_T) distributions of the Z boson provides new information about the dynamics of proton collisions at high energies. The y distribution of Z bosons is sensitive to the PDFs, particularly when measured in the forward region ($|y| > 2.5$), as done in this paper. The q_T spectrum provides a better understanding of the underlying collision process at low transverse momentum, and tests NNLO perturbative QCD predictions at high transverse momentum.

The rapidity is defined as $y = \frac{1}{2}\ln\left[(E + q_L)\,/\,(E - q_L)\right]$, where E is the energy of the Z-boson candidate and q_L is its longitudinal momentum along the anti-clockwise beam axis (the z axis of the detector). The Z-boson y and q_T are determined from the lepton momenta, which can be measured with high precision in the CMS detector. The measured differential dimuon and dielectron cross sections are normalized to the inclusive Z cross section, thereby canceling several sources of systematic uncertainties.

The Z-boson y and q_T distributions have been measured by the Tevatron experiments [5–8]. In this paper, we report measurements which cover the range in rapidity up to 3.5 and in transverse momentum up to 600 GeV, a similar range to results recently reported by the ATLAS experiment [9, 10]. The rapidity measurement is sensitive to the PDFs for proton momentum fractions (x) between 4×10^{-4} and 0.43.

2 The CMS detector

The central feature of the CMS apparatus is a superconducting solenoid of 6 m internal diameter, providing a magnetic field of 3.8 T. Within the field volume are a silicon pixel and strip tracker, a crystal electromagnetic calorimeter (ECAL), and a brass/scintillator hadron calorimeter (HCAL). The inner tracker measures charged particle trajectories in the pseudorapidity range $|\eta| < 2.5$ and provides a transverse momentum (p_T) resolution of about 1–2% for charged particles with p_T up to 100 GeV. The pseudorapidity η is defined as $\eta = -\ln(\tan(\theta/2))$, where θ is the polar angle with respect to the anti-clockwise beam direction. The electromagnetic calorimeter contains nearly 76 000 lead-tungstate crystals that provide a coverage of $|\eta| < 1.48$ in a cylindrical barrel region and of $1.48 < |\eta| < 3.0$ in two endcap regions. The ECAL has an energy resolution of better than 0.5% for unconverted photons with transverse energies above 100 GeV. The energy resolution is 3% or better for electrons with $|\eta| < 2.5$. The regions

($3.0 < |\eta| < 5.0$) are covered by sampling Cherenkov calorimeters (HF) constructed with iron as the passive material and quartz fibers as the active material. The HF calorimeters have an energy resolution of about 10% for electron showers. Muons are detected in the range $|\eta| < 2.4$, with detection planes based on three technologies: drift tubes, cathode strip chambers, and resistive plate chambers. Matching segments from the muon system to tracks measured in the inner tracker results in a p_T resolution of between 1 and 5% for muons with p_T up to 1 TeV. Data are selected online using a two-level trigger system. The first level, consisting of custom hardware processors, selects events in less than 1 μs, while the high-level trigger processor farm further decreases the event rate from around 100 kHz to about 300 Hz before data storage. A more detailed description of CMS can be found in Ref. [11].

3 Analysis procedure, data samples, and event selection

The differential cross section is determined in each y or q_T bin by subtracting from the number of detected events in a bin the estimated number of background events. The distributions are corrected for signal acceptance and efficiency and for the effects of detector resolution and electromagnetic final-state radiation (FSR) using an unfolding technique based on the inversion of a response matrix. The final result takes into account the bin width and is normalized by the measured total cross section.

The measurements of the rapidity and transverse momentum spectra are based on samples of over 12 000 Z-boson events reconstructed in each dilepton decay mode, and collected using high p_T single-lepton triggers. The lepton identification requirements used in the analysis are the same as those employed in the measurement of the inclusive W and Z cross sections [12]. For the Z-boson candidates selected, the pairs of leptons, ℓ, are required to have a reconstructed invariant mass in the range $60 < M_{\ell\ell} < 120$ GeV.

Muon events are collected using a trigger requiring a single muon, with a p_T threshold that was increased from 9 to 15 GeV in response to increasing LHC luminosity during the data-taking period. The two muon candidates with the highest p_T in the event are used to reconstruct a Z-boson candidate. Muons are required to have $p_T > 20$ GeV, $|\eta| < 2.1$, and to satisfy the standard CMS muon identification criteria described in Ref. [12]. In addition, the two muons are required to be isolated by calculating the sum of additional track momenta (I_{trk}) and hadron calorimeter energy not associated with the muon (I_{HCAL}) in a cone $\Delta R = \sqrt{(\Delta\eta)^2 + (\Delta\phi)^2} < 0.3$ around the muon momentum direction, and requiring $(I_{trk} + I_{HCAL})/p_T(\mu) < 0.15$. Information from the ECAL is not used as a criterion for isolation to avoid dependencies on FSR modeling [4]. At least one of the reconstructed muons must have triggered the event. The two muons in a pair are required to have opposite charges as determined by track curvature. The invariant mass distribution for selected events is shown in Fig. 1. We compare the kinematic distributions from the data and the simulations described below, and find that they agree.

Electrons are detected in either the ECAL or the HF. For this analysis, the acceptance for electrons is defined to be within the fiducial region of ECAL, which overlaps with the silicon tracker region, or in the fiducial region of the HF. Electrons in this analysis can thus be observed over pseudorapidity ranges of $|\eta| < 1.444$ (ECAL barrel), $1.566 < |\eta| < 2.5$ (ECAL endcaps), and $3.1 < |\eta| < 4.6$ (HF). The invariant mass distributions for selected events in the ECAL-ECAL and the ECAL-HF case are shown separately in Fig. 1. Events are selected online by a trigger requiring a single electron in the ECAL with $p_T \geq 17$ GeV. The two electron candidates with highest p_T in the event are used to reconstruct a Z-boson candidate, and at least one electron must be in the ECAL and have triggered the event. No requirement is applied on the charges of the electrons. Electrons are required to have $p_T \geq 20$ GeV. Electrons reconstructed in the

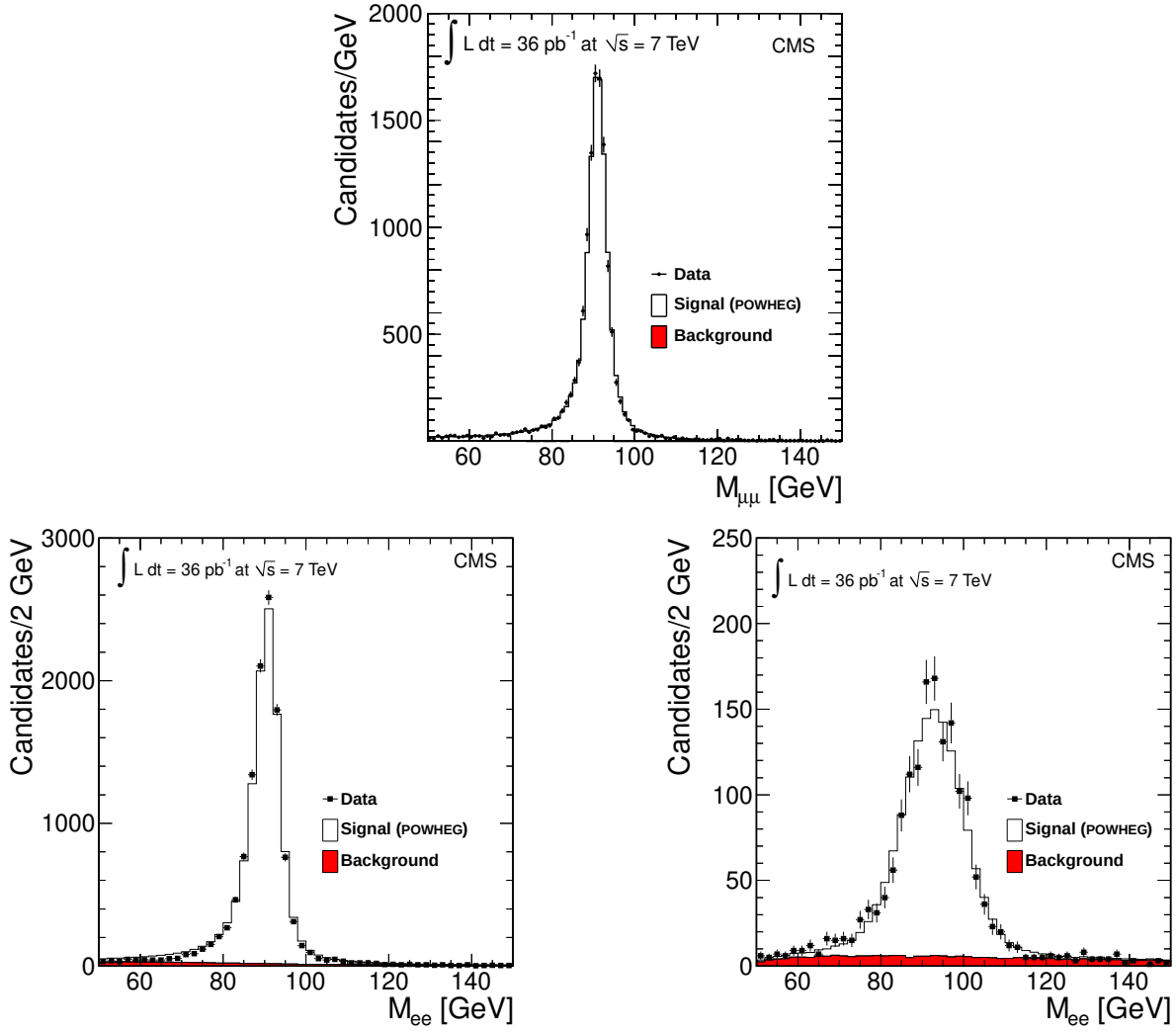

Figure 1: Dilepton invariant mass distributions for the muon channel (top) and the electron channel (bottom). The bottom-left plot for the electron shows the invariant mass distribution for events with both electrons in the ECAL and the bottom-right for events with one electron in the ECAL and the other in the HF. Each plot shows the data observation compared to the signal as predicted by POWHEG on top of the background estimated from a combination of simulation and data. The background is very low in the muon channel.

ECAL must have a matching track pointing to the reconstructed electromagnetic cluster and to be isolated and satisfy the general CMS electron identification criteria as described in Ref. [12].

Electrons are reconstructed in the HF calorimeters from clusters of 3-by-3 towers centered on a seed tower with $p_{\mathrm{T}} > 5\,\mathrm{GeV}$. Each tower provides both a measurement of total energy deposited and the energy deposited after the 12.5 radiation lengths (22 cm) of absorber closest to the interaction region. The two measurements are approximately equal for high-energy hadrons, while for electromagnetic particles the second measurement is typically a third of the total measured energy. Spurious signals from particles which pass directly through the phototube windows of the HF are rejected by requiring that the energy be shared among multiple towers. Electromagnetic clusters are selected by requiring the energy in the cluster to be at least 94% of the energy in the 5-by-5-tower region containing the cluster. A further selection is performed using the ratio of the two energy measurements and the ratio of the two most energetic towers in the cluster to the total cluster energy.

The detector acceptance is obtained from the simulation of the Drell–Yan process generated with the POWHEG [13] matrix-element NLO generator interfaced with the PYTHIA (v. 6.422) [14] parton-shower event generator, using the CT10 parametrization of the PDFs [15] and the Z2 underlying event tune [16]. The Z2 tune is the standard for CMS simulation and was tuned to the observed minimum-bias and underlying event characteristics at $\sqrt{s} = 7\,\mathrm{TeV}$ [17]. The effect of FSR is simulated using PYTHIA. In the muon channel, acceptance and efficiency calculations for the signal are performed using the full GEANT4-based [18] detector simulation, with additional smearing added to correct for observed differences in resolution between data and simulation as discussed below. For the electron channel, a parametrized simulation, matched to the resolution of the detector as measured in data, was used for efficiency and acceptance calculations. For the q_{T} measurement, the electron acceptance is restricted to $|\eta| < 2.1$ to match the muon acceptance.

The individual lepton detection and selection efficiencies are determined using a "tag-and-probe" method on the candidate lepton pairs. One of the leptons of the pair, the "tag", is required to pass all the selection requirements. The other lepton, the "probe", is selected with all requirements in the selection up to but excluding the requirement under study. The lepton pair is required to have an invariant mass consistent with the Z boson. When multiple tag-probe combinations are possible in a given event, one is chosen at random. The fraction of the probe leptons that also meet the requirement under study determines the efficiency of the requirement, after subtraction of the background from both samples using a fit to the dilepton invariant mass. In this manner, the efficiencies for the reconstruction, isolation, and trigger are measured sequentially. These efficiencies are compared with the efficiencies determined from the simulation to produce correction factors, some of which depend on the lepton kinematics, as discussed below. The efficiencies for an electron to form a cluster and a muon to form a basic track, both of which are very high, are taken from the GEANT4 simulation, which includes a modeling of inactive detector regions. The product of efficiency and acceptance for a given bin of y or q_{T} is determined using Monte Carlo simulation as the ratio of the number of generated events reconstructed in the bin to the number of generated events before the FSR correction, using the single-lepton efficiencies determined from data.

The single-muon trigger efficiency is determined separately for the different data-taking periods and varies from 0.880 ± 0.008 at the beginning of the period to 0.924 ± 0.003 at the end. The single-muon trigger efficiencies are shown to be independent of p_{T} and η within the acceptance used in this analysis. The trigger efficiency for events with two muons of $p_{\mathrm{T}} > 20\,\mathrm{GeV}$ and $|\eta| < 2.1$ is 0.993 ± 0.005, averaged over data-taking periods. The average muon recon-

struction and identification efficiency for the selection used in this analysis is 0.950 ± 0.003. The uncertainty on the efficiencies is dominated by the data sample size for the tag-and-probe measurement.

The single-electron trigger efficiency is measured to be between 0.96 ± 0.03 and 0.99 ± 0.01, varying as a function of p_T and η. For events with both electrons in the ECAL, the event trigger efficiency is greater than 0.999. For the electron channel, the total reconstruction and identification efficiencies determined from data range between 0.50 and 0.90 and are applied to the simulation as functions of p_T and η. Typical reconstruction and identification efficiency uncertainties are between 1 and 10%. However, the impact of these uncertainties on the final measurement uncertainty is greatly reduced by the normalization to the total cross section.

The main sources of background in the measurement are $Z \to \tau\tau$ and QCD multijet, $t\bar{t}$, W + jets, and diboson production. Diboson production including a Z is considered to be a background for the measurement. All backgrounds except for QCD multijet production are evaluated using Monte Carlo simulation. The $Z \to \tau\tau$ events are generated with POWHEG+PYTHIA. Events from $t\bar{t}$, diboson production, and W + jets are generated using the MADGRAPH (v. 4.4.12) [19] matrix-element generator interfaced to PYTHIA. Generated events are processed through the full GEANT4-based detector simulation, trigger emulation, and event reconstruction chain. We validated the use of the simulation to determine the background from the $Z \to \tau\tau$, $t\bar{t}$, and diboson backgrounds by analyzing the q_T spectrum for the eμ pairs. These background processes are flavor-symmetric and produce twice as many eμ pairs as ee or $\mu\mu$ pairs. The analysis of this data sample matched the expectation from simulation.

The QCD background is estimated using collision data samples. In the muon channel, the QCD background is estimated using a nonisolated dimuon sample corrected for the small contributions in the nonisolated sample from prompt muons such as those from $t\bar{t}$ or Z-boson decay. The estimate is verified using a like-sign dimuon sample, since nonprompt sources of dimuons should have equal rates of like-sign and opposite-sign events. The QCD background in the muon channel is found to be very small. In the electron channel, the QCD background is larger and can be directly estimated by fitting the dielectron mass distributions in the data. The fit was performed in each measurement bin over the range $40 < M_{ee} < 140\,\text{GeV}$ using a linear combination of a signal shape from simulation and a background shape determined by inverting the isolation and electron identification requirements in the data selection.

After applying all analysis selection criteria, the total background fraction in the muon channel is $0.4 \pm 0.4\%$, consisting primarily of $Z \to \tau\tau$ and $t\bar{t}$ processes and with an uncertainty dominated by statistical uncertainties in the background simulation. In the electron channel, the background fraction is $1.0 \pm 0.5\%$ for Z bosons reconstructed using two electrons in ECAL and $10 \pm 4\%$ for Z bosons reconstructed using one electron in ECAL and one in the HF, where the uncertainty is dominated by statistical uncertainties in the QCD estimate. In the electron channel, the QCD background is the dominant background component in every bin of rapidity and also at low q_T. In the highest four q_T bins, the $Z \to \tau\tau$ and $t\bar{t}$ processes are the dominant contributions to the background.

The bin width in rapidity ($\Delta y = 0.1$) is chosen to allow a comparison with previous measurements at lower center-of-mass energies. The bin widths in q_T, which vary from 2.5 to 350 GeV, are chosen to provide sufficient resolution to observe the shape of the distribution, to limit bin migration, and to ensure a sufficient data sample in each measurement bin.

The final measured y and q_T distributions are corrected for bin-migration effects arising from the detector resolution and from FSR using a matrix-based unfolding procedure [20]. Large

simulation samples are used to create the response matrices, which are inverted and used to unfold the measured distribution. This unfolding is applied to allow the combination of the muon and electron channels, which have different resolutions, and to allow the comparison with results from other experiments. The corrections resulting from detector resolution are calculated by comparing the generator-level dilepton distribution after FSR obtained from POWHEG+PYTHIA to that of the reconstructed simulated events, after smearing the momentum of each lepton with a parametrized function. The function is derived by comparing the Z mass distribution in data and the Monte Carlo detector simulation for different regions of η and p_{T}. In the muon channel, the smearing represents the observed difference between the resolution in data and in simulation. In the electron channel, as described above, a fully parametrized simulation is used for the acceptance and efficiency corrections. The corrections due to FSR are based on a Monte Carlo simulation using PYTHIA, and are obtained by comparing the dilepton y and q_{T} distributions before and after FSR. These corrections are primarily important for the muon measurements, though large-angle FSR also has an impact on the electron distributions.

4 Systematic uncertainties

The leading sources of systematic uncertainty for the normalized distribution measurements are the background estimates, the trigger and identification efficiencies, the unfolding procedure, the calorimeter energy scale, and the tracker misalignment. Since the measurements are normalized by the total measured cross sections, several sources of systematic uncertainty cancel, as they affect both the total rate and the differential rate in the same manner. For example, the uncertainty in the luminosity measurement cancels completely and uncertainties resulting from the lepton efficiencies and from the PDFs are significantly reduced.

The muon and electron measurements share several theory-dependent uncertainties. Given the importance of the rapidity measurement in constraining PDFs, it is crucial to estimate the effect of the uncertainties in the PDFs on the determination of the bin-by-bin acceptance for the measurement. To evaluate the effect, we use the variations provided as part of the CT10 PDF set [15]. For this PDF set, 52 variations are provided, each of which represents a shift in the PDFs by plus or minus one standard deviation along one of the 26 eigenvectors of the model. These eigenvectors are used to parametrize the uncertainties of the PDFs by diagonalizing the actual PDF model fit parameters, taking into account the unitary requirement and other constraints. The eigenvectors are not simply connected to specific observables, but represent an orthogonal basis in the PDF model space along which the uncertainties can be calculated. For each variation, the effect on the bin-by-bin acceptance normalized by the total acceptance was determined. The effects are combined in quadrature for each bin, separating negative and positive effects, to give the total uncertainty. The resulting uncertainties in the acceptance are less than 0.2% over the entire measurement range. However, the change in the shape of the distributions as a function of y is quite significant, up to 4% at high rapidity for some variations. These changes do not represent systematic uncertainties in the measurement – instead they represent the sensitivity of the analysis for constraining the PDFs.

Several background processes, as described in Section 3, are predicted from Monte Carlo simulation and compared with the data. A conservative estimate of the possible impact on the measurement is derived by varying the estimates of the small background from these sources by 100% based on the uncertainty due to the limited simulation sample size. We calculate the deviation of the central value of the normalized distribution in each bin when the background levels are varied. For the electron channel, the estimation of the bin-by-bin QCD background from data is a leading source of systematic uncertainty. Here, the error on the level of back-

Table 1: Fractional systematic uncertainty contributions for representative rapidity bins and transverse momentum bins in the electron and muon channels.

$\lvert y\rvert$ Range	$[0.0, 0.1]$		$[1.8, 1.9]$		$[3.0, 3.1]$
Channel	Muon	Electron	Muon	Electron	Electron
Background Estimation	0.002	0.010	0.002	0.015	0.047
Efficiency Determination	0.003	0.005	0.007	0.007	0.047
Energy/Momentum Scale	0.001	0.004	0.001	0.003	0.009
PDF Acceptance Determination	0.001	0.001	0.001	0.001	0.001
Total	0.004	0.012	0.007	0.017	0.067

q_{T} Range	$[2.5\,\mathrm{GeV}, 5.0\,\mathrm{GeV}]$		$[110\,\mathrm{GeV}, 150\,\mathrm{GeV}]$	
Channel	Muon	Electron	Muon	Electron
Background Estimation	0.004	0.005	0.019	0.028
Efficiency Determination	0.010	0.002	0.010	0.008
Energy Scale	–	0.022	–	0.035
Tracker Alignment	0.015	0.013	0.023	0.020
Unfolding	0.006	0.004	0.017	0.001
PDF Acceptance Determination	0.002	0.002	0.001	0.001
Total	0.020	0.026	0.036	0.050

ground in the signal region, $60 < M_{\mathrm{ee}} < 120\,\mathrm{GeV}$, is dominated by the lack of data available in the dilepton invariant mass sideband regions.

The trigger and the identification efficiencies are measured in the data as described above. The largest uncertainty in the efficiencies arises from the size of the data sample. To estimate the impact of these uncertainties on the final measurement, we change the efficiencies by plus or minus the amount of their statistical uncertainties and determine the changes of the normalized distribution. The changes from the central value are assigned as the systematic uncertainty arising from the efficiency measurements, taking into account the cancellation effect from the rate normalization. The efficiencies from each stage of the selection are considered independently, and the resulting uncertainties are summed in quadrature.

The systematic uncertainty from the unfolding procedure is estimated using alternative response matrices derived in several ways. We consider different generator models for the q_{T} spectrum, which can affect the distribution of events within the bins. We vary the parameters of the detector resolution functions within their uncertainties. We also reweight the smeared spectrum to match the data and evaluate the differences between the nominal and the reweighted unfolded spectra. In all cases, the effects amount to less than 0.5%.

For the electron channel, the imperfect knowledge of the absolute and relative energy scales in the electromagnetic and forward calorimeters is a source of systematic uncertainty. Using Monte Carlo simulations, we estimate the effect of the scale uncertainties by scaling the energies of electrons by amounts corresponding to the calibration uncertainties and the difference observed between the different calibration techniques used in the calorimeters. These energy scale uncertainties depend on the position of the electron within the calorimeters. We then determine the impact of these shifts on the observed distributions.

The muon p_{T} used in the analysis is based on the silicon tracker measurement. Thus, any misalignment of the tracker may directly affect the muon momentum resolution. The systematic uncertainty associated with tracker misalignment is calculated by reprocessing the Drell–Yan

simulation using several models designed to reproduce the possible misalignments that may be present in the tracker. The bin-by-bin maximum deviation from the nominal Drell–Yan simulation is used as estimator of the tracker misalignment uncertainty. In the electron channel, the sensitivity to the tracker alignment is determined by comparing the reconstructed y and p_{T} using the calorimeter energy alone with those including the track measurements, for both data and simulation.

The systematic uncertainties are summarized in Table 1 for representative values of y and q_{T} in the muon and electron channels. After combining the effects discussed above, the total systematic uncertainty in each bin is found to be significantly smaller than the statistical uncertainty.

5 Rapidity Distribution Results

The rapidity y of Z bosons produced in proton-proton collisions is related to the momentum fraction x_+ (x_-) carried by the parton in the forward-going (backward-going) proton as described by the leading-order formula $x_\pm = \frac{m_Z}{\sqrt{s}} e^{\pm y}$. Therefore, the rapidity distribution directly reflects the PDFs of the interacting partons. At the LHC, the rapidity distribution of Z bosons is expected to be symmetric around zero, therefore the appropriate measurement is the distribution of Z bosons as a function of the absolute value of rapidity. The measurement is normalized to the total cross section ($1/\sigma \; d\sigma/d\,|y|$), where σ is the cross section determined by the sum of all observed y bins ($|y| < 3.5$), corrected to the total cross section as calculated from POWHEG with CT10 PDFs. The calculated correction between the measured and total y range is 0.983 with an uncertainty of 0.001 from PDF variation.

The measurements for the muon and electron channels are given in Table 2 and are in agreement with each other (reduced $\chi^2 = 0.85$) over the 20 bins where the measurements overlap. We combine these two measurements using the procedure defined in Ref. [21], which provides a full covariance matrix for the uncertainties. The uncertainties are considered to be uncorrelated between the two analyses, since the only correlation between the channels is from the small PDF uncertainty. The combined measurements are shown in Table 2 and compared to the predictions made using CT10 PDFs in Fig. 2.

To evaluate the sensitivity of this result to parameters of some of the more-recent PDF sets, we determine the change in the χ^2 for each variation of the eigenvectors provided in the PDF sets. The CT10 PDF set has a χ^2 of 18.5 for the base prediction, and the eigenvector-dependent changes in χ^2 are shown in Fig. 3. The number of degrees of freedom (ndof) is 34. The MSTW2008 [22] PDF set has a χ^2 of 18.3 for its base prediction, and the eigenvector-dependent changes shown in Fig. 4. For both sets, several eigenvectors show significant sensitivity to our result, with CT10 showing a generally larger sensitivity. The HERAPDF 1.5 [23] PDF set, which has a χ^2 of 18.4 for its base prediction, provides both eigenvectors and model dependencies as part of the PDF set. The changes in χ^2 for both are shown in Fig. 5. The largest model dependencies with our measurement are the strange-quark PDF as a fraction of the down-quark-sea PDF. For the NNPDF 2.0 PDF set [24], the base prediction has a χ^2 of 18.4. The NNPDF formalism does not use eigenvectors, but rather replica PDFs sampled from the same space. In comparing our result with the 100 standard NNPDF 2.0 replicas, the majority have χ^2 similar to the base, but some have χ^2 values up to 34.5, indicating that these replicas are disfavored significantly by the new measurement.

Table 2: Measurement of the normalized differential cross section $\left(\frac{1}{\sigma}\frac{\mathrm{d}\sigma}{\mathrm{d}|y|}\right)$ for Drell–Yan lepton pairs in the Z-boson mass region ($60 < M_{\ell\ell} < 120\,\mathrm{GeV}$) as a function of the absolute value of rapidity, separately for the muon and electron channels and combined. Detector geometry and trigger uniformity requirements limit the muon channel measurement to $|y| < 2.0$. The uncertainties shown are the combined statistical and systematic uncertainties.

	Normalized Differential Cross section		
$\lvert y\rvert$ Range	Muon	Electron	Combined
$[0.0, 0.1]$	0.324±0.012	0.359±0.015	0.337±0.010
$[0.1, 0.2]$	0.338±0.013	0.326±0.016	0.335±0.010
$[0.2, 0.3]$	0.338±0.013	0.344±0.017	0.341±0.010
$[0.3, 0.4]$	0.341±0.013	0.355±0.017	0.346±0.010
$[0.4, 0.5]$	0.363±0.013	0.339±0.017	0.354±0.011
$[0.5, 0.6]$	0.342±0.013	0.351±0.018	0.346±0.010
$[0.6, 0.7]$	0.312±0.013	0.360±0.018	0.328±0.010
$[0.7, 0.8]$	0.354±0.013	0.331±0.018	0.347±0.011
$[0.8, 0.9]$	0.343±0.014	0.355±0.018	0.347±0.011
$[0.9, 1.0]$	0.332±0.014	0.332±0.018	0.332±0.011
$[1.0, 1.1]$	0.336±0.014	0.316±0.018	0.329±0.011
$[1.1, 1.2]$	0.324±0.014	0.352±0.019	0.334±0.011
$[1.2, 1.3]$	0.321±0.014	0.332±0.019	0.325±0.011
$[1.3, 1.4]$	0.355±0.016	0.321±0.019	0.341±0.012
$[1.4, 1.5]$	0.326±0.016	0.313±0.019	0.319±0.012
$[1.5, 1.6]$	0.331±0.018	0.330±0.020	0.330±0.013
$[1.6, 1.7]$	0.294±0.018	0.306±0.022	0.299±0.014
$[1.7, 1.8]$	0.331±0.021	0.332±0.024	0.331±0.016
$[1.8, 1.9]$	0.324±0.025	0.294±0.024	0.308±0.017
$[1.9, 2.0]$	0.328±0.032	0.328±0.026	0.328±0.020
$[2.0, 2.1]$		0.294±0.027	0.294±0.027
$[2.1, 2.2]$		0.298±0.029	0.298±0.029
$[2.2, 2.3]$		0.290±0.031	0.290±0.031
$[2.3, 2.4]$		0.278±0.035	0.278±0.035
$[2.4, 2.5]$		0.199±0.038	0.199±0.038
$[2.5, 2.6]$		0.249±0.040	0.249±0.040
$[2.6, 2.7]$		0.241±0.037	0.241±0.037
$[2.7, 2.8]$		0.256±0.035	0.256±0.035
$[2.8, 2.9]$		0.221±0.034	0.221±0.034
$[2.9, 3.0]$		0.165±0.035	0.165±0.035
$[3.0, 3.1]$		0.183±0.040	0.183±0.040
$[3.1, 3.2]$		0.228±0.045	0.228±0.045
$[3.2, 3.3]$		0.078±0.043	0.078±0.043
$[3.3, 3.4]$		0.105±0.051	0.105±0.051
$[3.4, 3.5]$		0.089±0.062	0.089±0.062

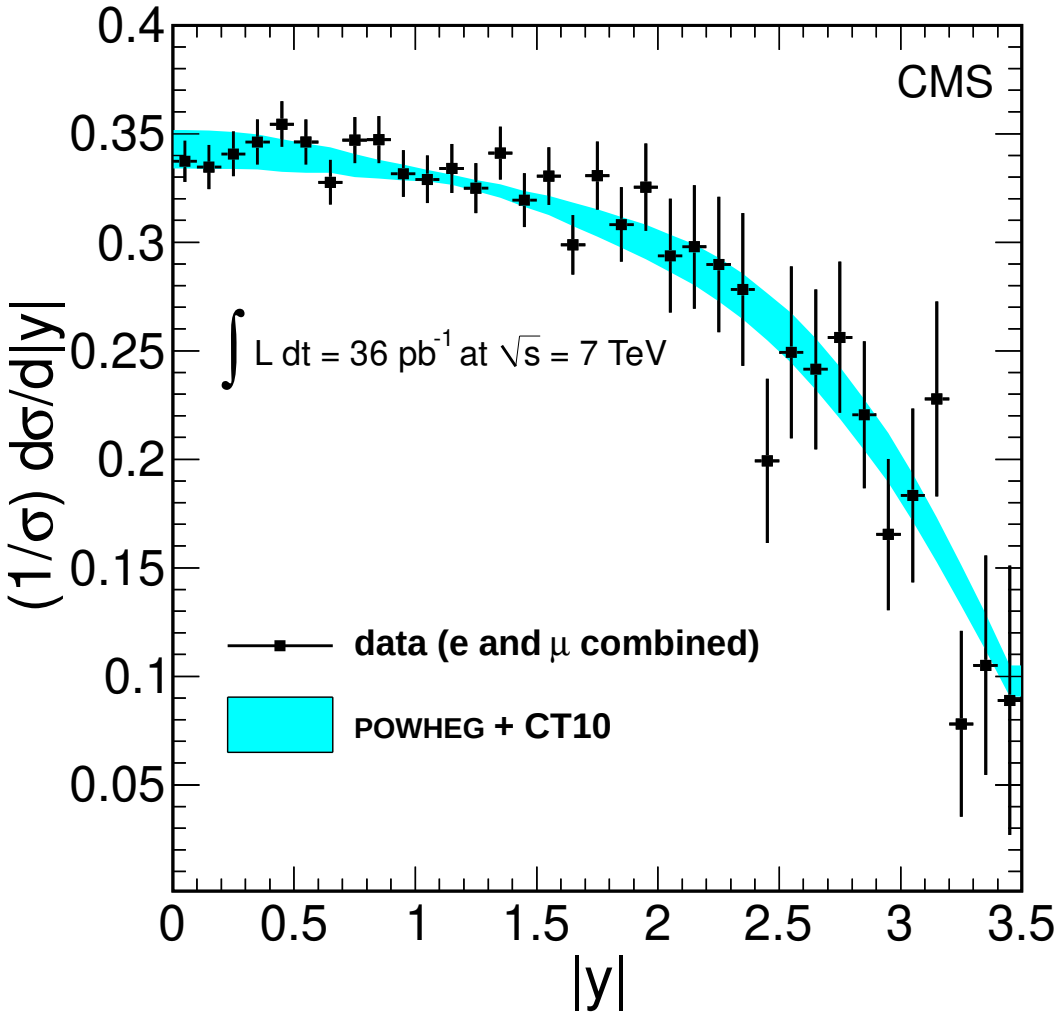

Figure 2: The normalized differential cross section for Z bosons as a function of the absolute value of rapidity, combining the muon and electron channels. The error bars correspond to the experimental statistical and systematic uncertainties added in quadrature. The shaded area indicates the range of variation predicted by the POWHEG simulation for the uncertainties of the CT10 PDFs.

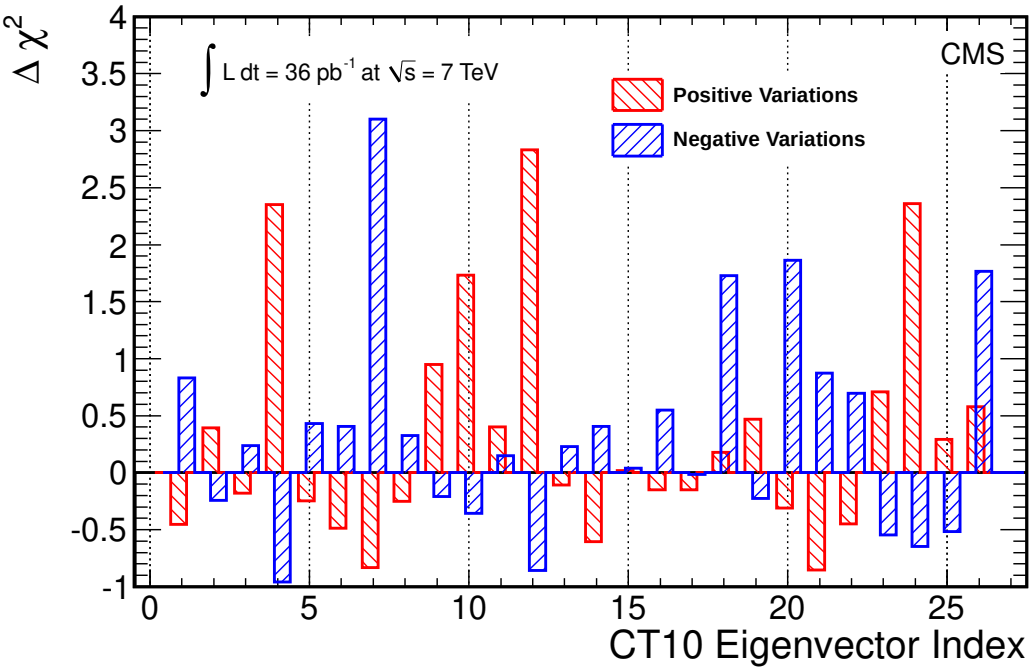

Figure 3: The change in χ^2 when comparing the Z rapidity differential cross section measurement with the predictions of the NLO CT10 PDF set as each of the eigenvector input parameters is varied by plus or minus one standard deviation around its default value.

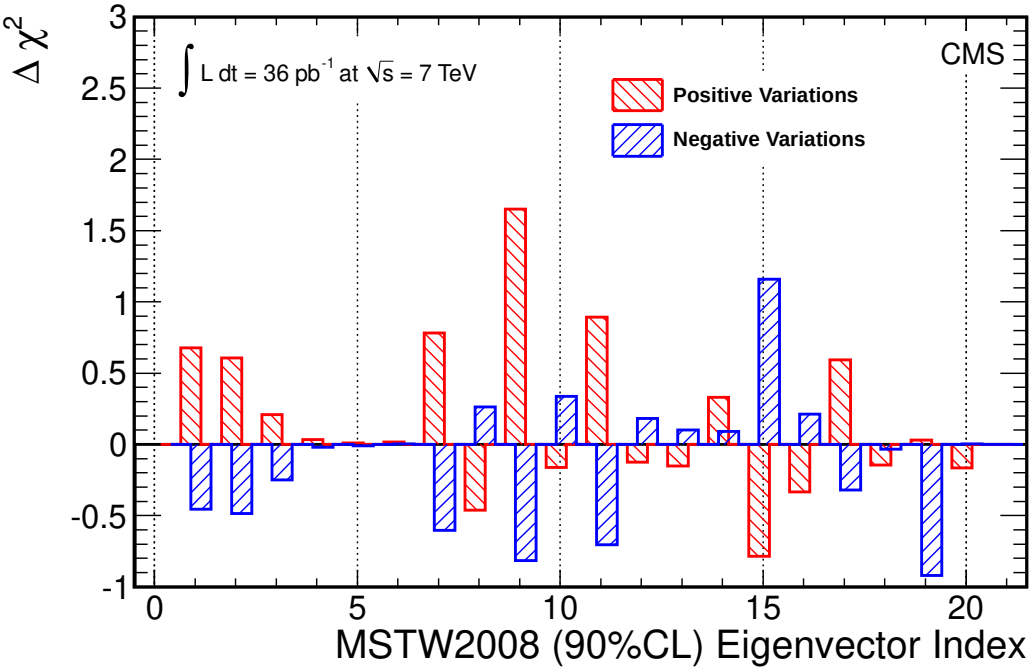

Figure 4: The change in χ^2 when comparing the Z rapidity differential cross section measurement with the predictions of the NLO MST2008 PDF set as each of the eigenvector input parameters is varied by $\pm$90% confidence level (CL) around its default value.

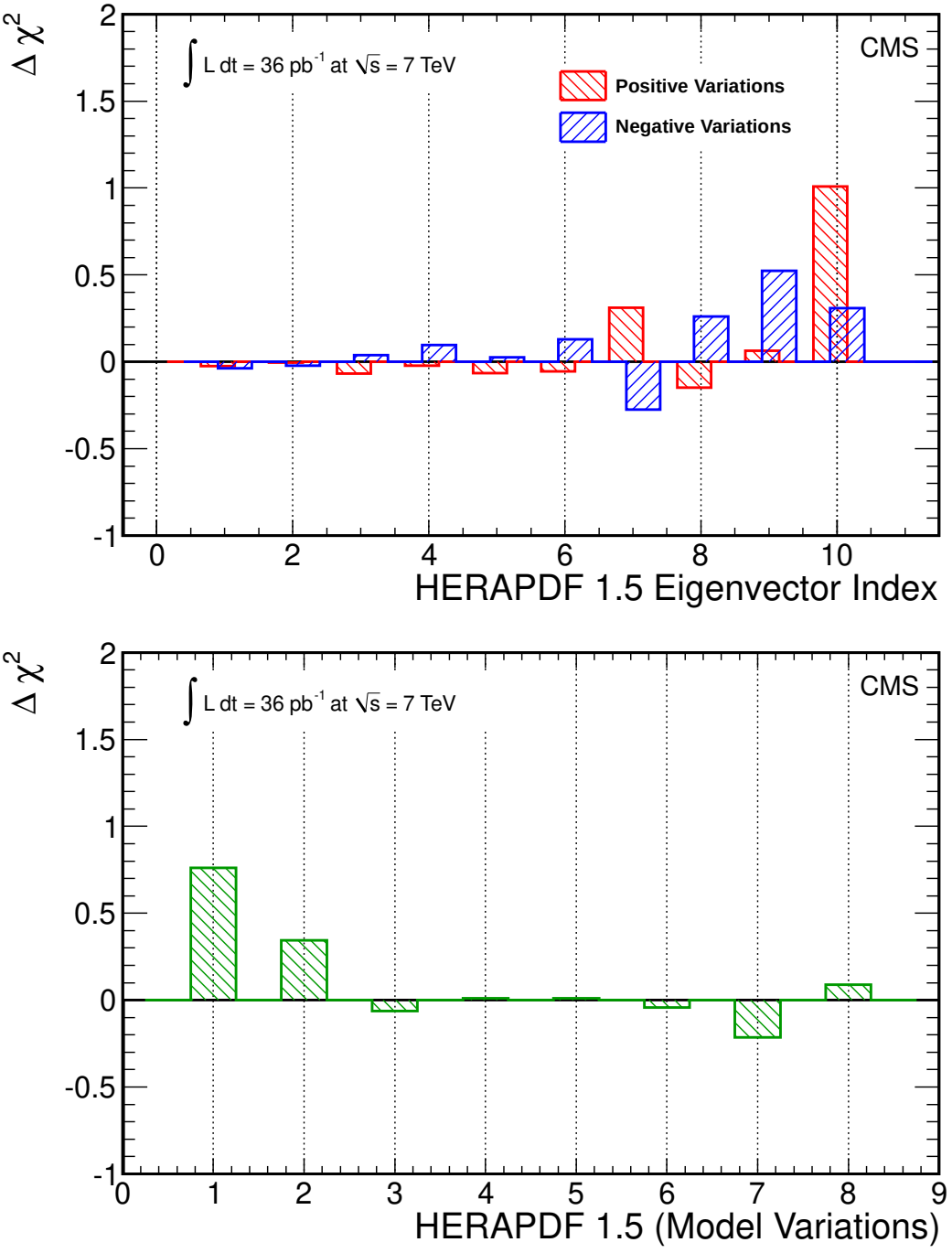

Figure 5: The change in χ^2 when comparing the Z rapidity differential cross section measurement with the predictions of the NLO HERAPDF 1.5 PDF set as each of the eigenvector input parameters (left) and the model parameters (right) is varied by one standard deviation around its default value. These together represent the full set of uncertainties in the HERAPDF 1.5 set.

6 Transverse Momentum Distribution Results

Measurements of the q_T distribution for Z bosons provide an important test of the QCD predictions of the initial-state gluon-radiation process. Perturbative QCD calculations are expected to provide a reliable prediction for the portion of the spectrum $q_T > 20\,\text{GeV}$, which is dominated by single hard-gluon emission. For $q_T < 10\,\text{GeV}$, the shape of the distribution is determined by multiple soft gluon radiation and nonperturbative effects. Such effects are simulated by Monte Carlo programs combining parton showering and parameterized models. These soft-gluon contributions can also be accounted for by resummation calculations in some Monte Carlo programs.

For the q_T measurement, the data are normalized to the cross section integrated over the acceptance region $|\eta| < 2.1$ and $p_T > 20\,\text{GeV}$. The lepton p_T and $|\eta|$ restrictions apply to both leptons of a dilepton pair. The restriction on the electron pseudorapidity (compared to that used for the rapidity measurement) allows the combination of the two channels and a more straightforward physics interpretation, as the two measurements refer to the same rapidity range and have the same PDF dependence.

Table 3: Measurement of the normalized differential cross section for Drell–Yan lepton pairs in the Z-boson mass region ($60 < M_{\ell\ell} < 120\,\text{GeV}$) as a function of q_T, separately for muon and electron channels and for the combination of the two channels. The distribution is normalized by the cross section for Z bosons with both leptons having $|\eta| < 2.1$ and $p_T > 20\,\text{GeV}$. The uncertainties listed in the table are the combined statistical and systematic uncertainties.

q_T Range (GeV)	Muon Channel	Electron Channel	Combination
[0.0, 2.5]	$(3.21 \pm 0.14) \times 10^{-2}$	$(3.24 \pm 0.25) \times 10^{-2}$	$(3.22 \pm 0.13) \times 10^{-2}$
[2.5, 5.0]	$(5.89 \pm 0.21) \times 10^{-2}$	$(6.03 \pm 0.32) \times 10^{-2}$	$(5.92 \pm 0.17) \times 10^{-2}$
[5.0, 7.5]	$(5.51 \pm 0.20) \times 10^{-2}$	$(5.32 \pm 0.32) \times 10^{-2}$	$(5.50 \pm 0.16) \times 10^{-2}$
[7.5, 10.0]	$(3.90 \pm 0.18) \times 10^{-2}$	$(4.20 \pm 0.30) \times 10^{-2}$	$(3.96 \pm 0.14) \times 10^{-2}$
[10.0, 12.5]	$(3.49 \pm 0.16) \times 10^{-2}$	$(3.60 \pm 0.28) \times 10^{-2}$	$(3.53 \pm 0.12) \times 10^{-2}$
[12.5, 15.0]	$(2.74 \pm 0.15) \times 10^{-2}$	$(2.70 \pm 0.25) \times 10^{-2}$	$(2.72 \pm 0.12) \times 10^{-2}$
[15.0, 17.5]	$(2.23 \pm 0.14) \times 10^{-2}$	$(2.00 \pm 0.22) \times 10^{-2}$	$(2.16 \pm 0.10) \times 10^{-2}$
[17.5, 20.0]	$(1.68 \pm 0.12) \times 10^{-2}$	$(1.59 \pm 0.20) \times 10^{-2}$	$(1.65 \pm 0.09) \times 10^{-2}$
[20.0, 30.0]	$(1.14 \pm 0.04) \times 10^{-2}$	$(1.20 \pm 0.05) \times 10^{-2}$	$(1.16 \pm 0.04) \times 10^{-2}$
[30.0, 40.0]	$(6.32 \pm 0.28) \times 10^{-3}$	$(5.62 \pm 0.31) \times 10^{-3}$	$(5.98 \pm 0.27) \times 10^{-3}$
[40.0, 50.0]	$(3.53 \pm 0.21) \times 10^{-3}$	$(3.18 \pm 0.24) \times 10^{-3}$	$(3.38 \pm 0.18) \times 10^{-3}$
[50.0, 70.0]	$(1.74 \pm 0.10) \times 10^{-3}$	$(1.90 \pm 0.12) \times 10^{-3}$	$(1.81 \pm 0.09) \times 10^{-3}$
[70.0, 90.0]	$(7.76 \pm 0.71) \times 10^{-4}$	$(7.86 \pm 0.77) \times 10^{-4}$	$(7.79 \pm 0.54) \times 10^{-4}$
[90.0, 110.0]	$(4.87 \pm 0.55) \times 10^{-4}$	$(4.57 \pm 0.59) \times 10^{-4}$	$(4.75 \pm 0.42) \times 10^{-4}$
[110.0, 150.0]	$(1.79 \pm 0.22) \times 10^{-4}$	$(2.18 \pm 0.26) \times 10^{-4}$	$(1.93 \pm 0.17) \times 10^{-4}$
[150.0, 190.0]	$(7.10 \pm 1.40) \times 10^{-5}$	$(4.82 \pm 1.31) \times 10^{-5}$	$(6.00 \pm 0.99) \times 10^{-5}$
[190.0, 250.0]	$(1.17 \pm 0.51) \times 10^{-5}$	$(2.05 \pm 0.64) \times 10^{-5}$	$(1.51 \pm 0.43) \times 10^{-5}$
[250.0, 600.0]	$(2.24 \pm 0.78) \times 10^{-6}$	$(0.81 \pm 0.52) \times 10^{-6}$	$(1.29 \pm 0.44) \times 10^{-6}$

The measurements from the muon and electron channels are tabulated in Table 3 and are found to be compatible with each other over the full q_T range (reduced $\chi^2 = 0.74$). The combination of the muon and electron results is also performed following Ref. [21]. The alignment uncertainty is treated as correlated between the two channels, and other uncertainties are treated as uncorrelated. The combined measurement is presented in Fig. 6, where the data points are positioned at the center-of-gravity of the bins, based on the POWHEG prediction. For

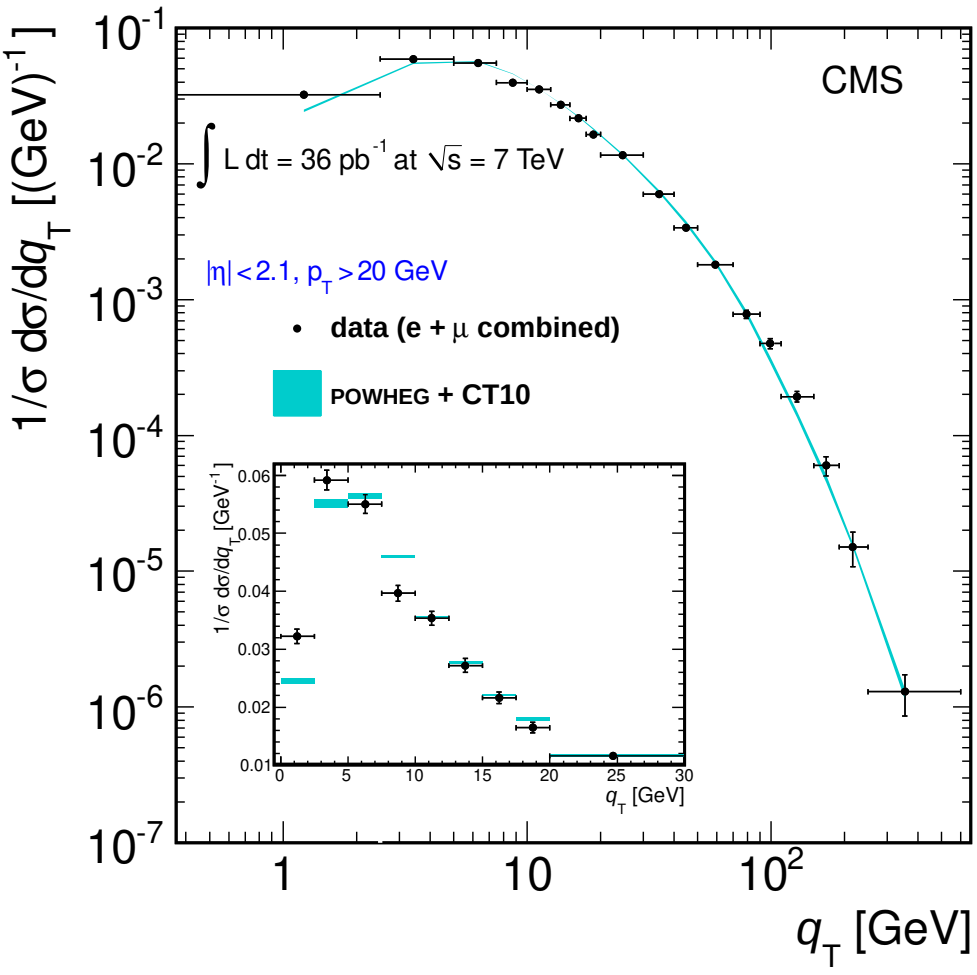

Figure 6: The Z-boson transverse momentum distribution found from combining the muon and electron channels, compared to the predictions of the POWHEG generator interfaced with PYTHIA using the Z2 tune. The error bars correspond to the statistical and systematic uncertainties added in quadrature. The band around the theoretical prediction includes the uncertainties due to scale variations and PDFs. The horizontal error bars indicate the bin boundaries, and the data points are positioned at the center-of-gravity of the bins, based on the POWHEG prediction. The inset figure shows the low q_{T} region on a linear scale.

$q_T > 20$ GeV, we compare the data and the prediction of POWHEG+PYTHIA with the Z2 tune and find $\chi^2/\text{ndof} = 19.1/9$, where ndof is equal to the number of points minus one because of the normalization. We have taken the full covariance matrix into account when computing the χ^2 values. At low momentum, there is poor agreement, suggesting the need for additional tuning of the combination of POWHEG and PYTHIA in this region, where both contribute to the observed q_T.

At low transverse momenta, i.e. $q_T < 30$ GeV, the distribution is determined by nonperturbative QCD, which is modeled by PYTHIA with a few free parameters. Several parameter sets called "tunes" are available, including the Perugia 2011 [25], ProQ20 [26], and Z2 tune [16]. The shapes predicted with these tunes are compared to this measurement in Fig. 7. Agreement is observed for the Z2 ($\chi^2/\text{ndof} = 9.4/8$) and the ProQ20 tunes ($\chi^2/\text{ndof} = 13.3/8$), but disagreement for the Perugia 2011 tune ($\chi^2/\text{ndof} = 48.8/8$) and for POWHEG+PYTHIA ($\chi^2/\text{ndof} = 76.3/8$). These results provide a validation of the Z2 tune for a high momentum-scale process that is rather different from the low-momentum-scale processes that determine the characteristics of minimum-bias events and the underlying event from which the parameters of the Z2 tune were originally obtained.

At high q_T, the precision of the prediction is dominated by the perturbative order of the calculation and the handling of the factorization and renormalization scale dependence. In Fig. 8 the measured normalized differential distribution is compared to the prediction of POWHEG as well as the "Fully Exclusive W, ZProduction" (FEWZ) package [27] for $q_T > 20$ GeV and $|\eta| < 2.1$, calculated at both $O(\alpha_s)$ and $O(\alpha_s^2)$. The predictions were each normalized to their own predicted total cross sections. The FEWZ calculation used the effective dynamic scale definition $\sqrt{M_Z^2 + \langle q_T \rangle^2}$ rather than the fixed scale of the Z-boson mass. The FEWZ $O(\alpha_s^2)$ prediction produces a χ^2/ndof of 30.5/9, which is a poorer agreement than the POWHEG prediction (19.1/9), particularly at the highest q_T.

7 Summary

Measurements of the normalized differential cross sections for Drell–Yan muon and electron pairs in the Z-boson mass region ($60 < M_{\ell\ell} < 120$ GeV) have been reported as functions of dilepton rapidity and transverse momentum separately. The results were obtained using a data sample collected by the CMS experiment at the LHC at a center-of-mass energy of 7 TeV corresponding to an integrated luminosity of 36 pb^{-1}. The rapidity measurement is compared with the predictions of several of the most recent PDF models and the agreement evaluated as a function of the PDF set eigenvectors. An overall agreement between the models and the data is observed. The measured transverse momentum distribution is compared to various tunes of the PYTHIA generator for low transverse momentum and to $O(\alpha_s)$ and $O(\alpha_s^2)$ predictions for high q_T. No single model describes the normalized differential cross section of the Z transverse momentum over the full range. These measurements significantly extend previous Tevatron results and complement recent LHC results in rapidity and transverse momentum.

Acknowledgments

We wish to congratulate our colleagues in the CERN accelerator departments for the excellent performance of the LHC machine. We thank the technical and administrative staff at CERN and other CMS institutes. This work was supported by the Austrian Federal Ministry of Science and Research; the Belgium Fonds de la Recherche Scientifique, and Fonds voor Wetenschappelijk

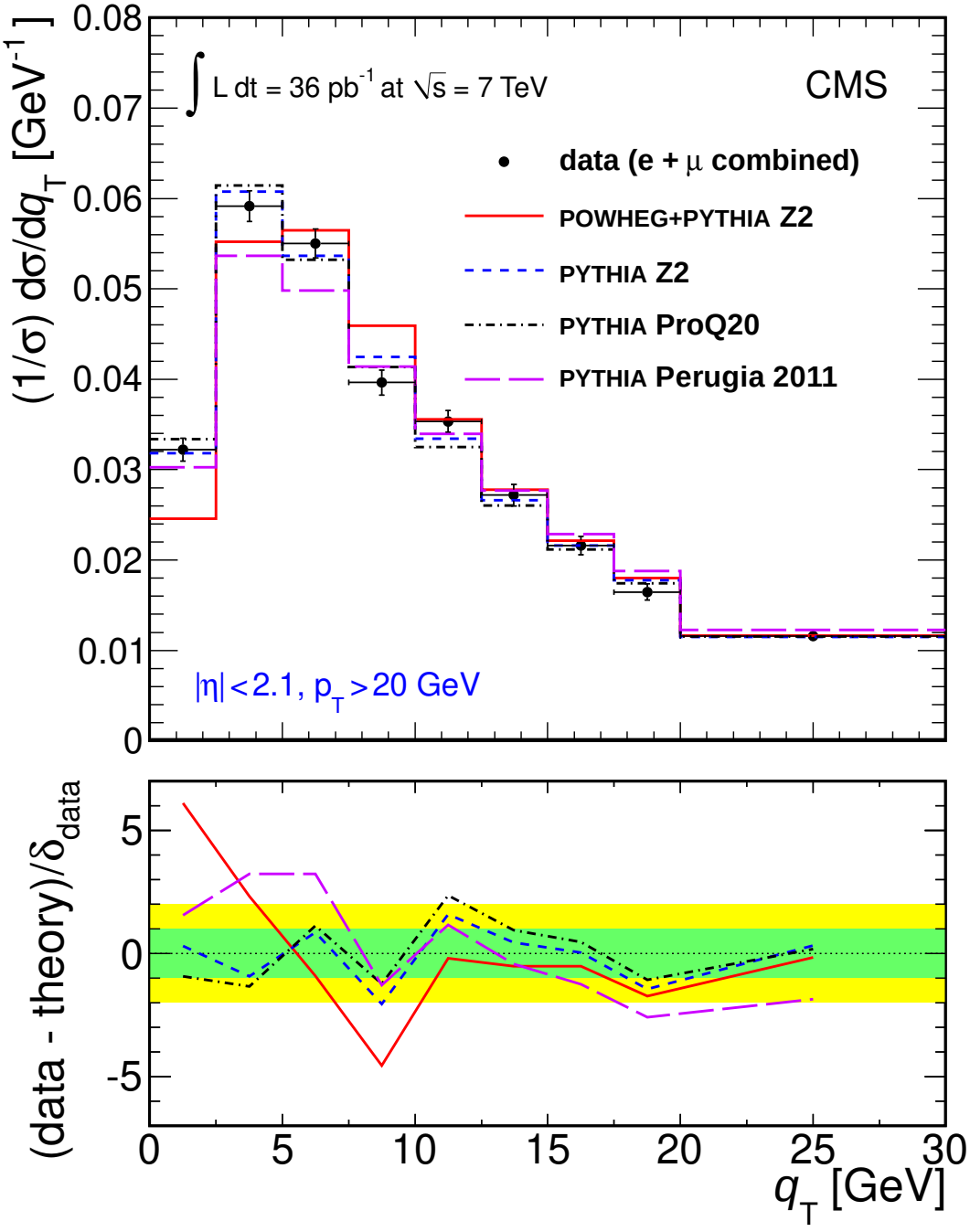

Figure 7: The combined electron and muon measurement of the Z-boson transverse momentum distribution (points) and the predictions of several PYTHIA tunes and POWHEG interfaced with PYTHIA using the Z2 tune (histograms). The error bars on the points represent the sum of the statistical and systematic uncertainties on the data. The lower portion of the figure shows the difference between the data and the simulation predictions divided by the uncertainty δ on the data. The green (inner) and yellow (outer) bands are the $\pm 1\delta$ and $\pm 2\delta$ experimental uncertainties.

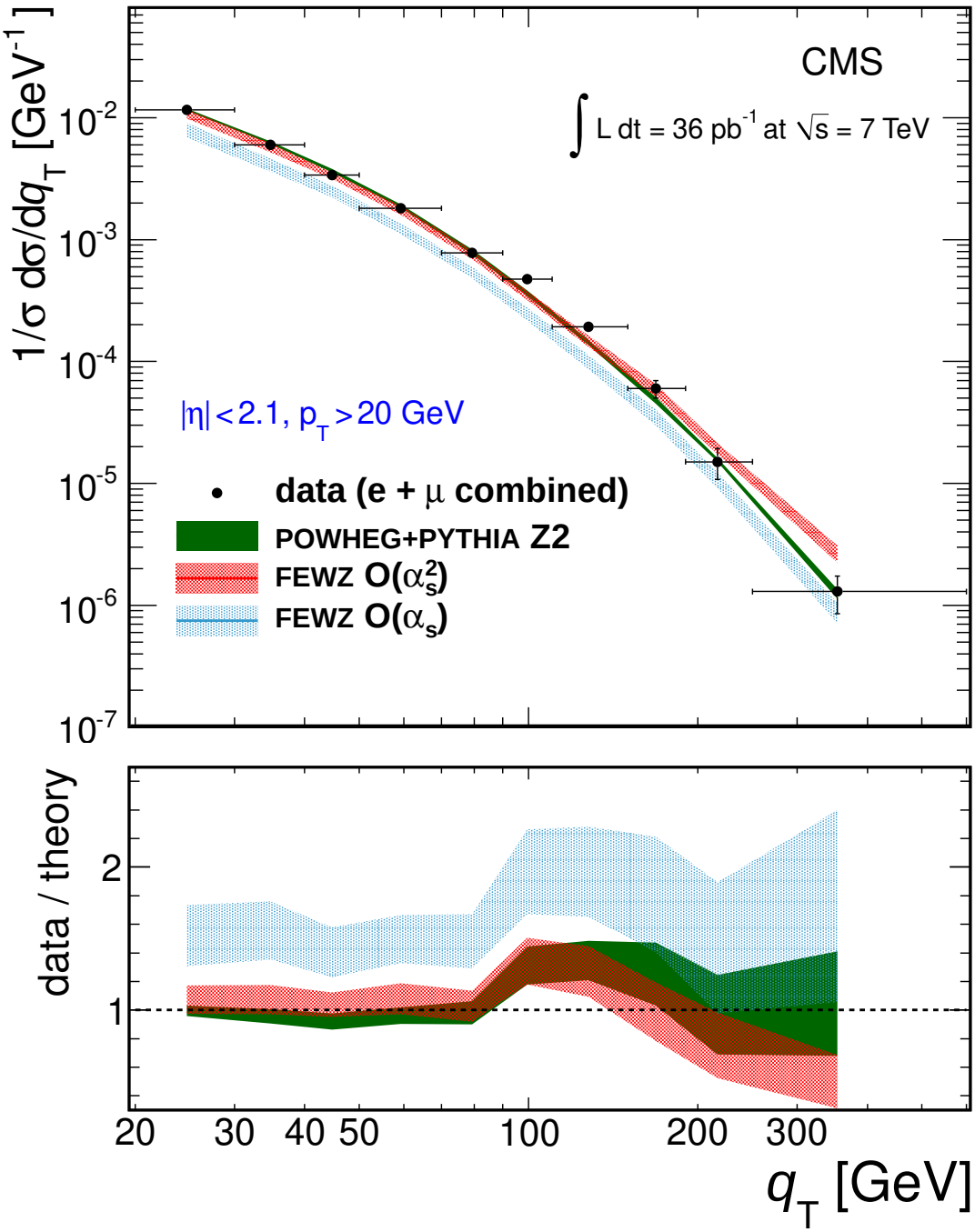

Figure 8: The combined electron and muon Z-boson normalized differential cross section as a function of transverse momentum (points) and the POWHEG and FEWZ predictions for $q_T > 20$ GeV. The horizontal error bars indicate the bin boundaries and the data points are positioned at the center-of-gravity of the bins based on the POWHEG prediction. The bands in the upper plot represent the uncertainty on the predictions from factorization and renormalization scales and PDFs. The lower plot shows the ratio between the data and the theory predictions. The bands in the lower plot represent the one standard deviation combined theoretical and experimental uncertainties.

Onderzoek; the Brazilian Funding Agencies (CNPq, CAPES, FAPERJ, and FAPESP); the Bulgarian Ministry of Education and Science; CERN; the Chinese Academy of Sciences, Ministry of Science and Technology, and National Natural Science Foundation of China; the Colombian Funding Agency (COLCIENCIAS); the Croatian Ministry of Science, Education and Sport; the Research Promotion Foundation, Cyprus; the Estonian Academy of Sciences and NICPB; the Academy of Finland, Finnish Ministry of Education and Culture, and Helsinki Institute of Physics; the Institut National de Physique Nucléaire et de Physique des Particules / CNRS, and Commissariat à l'Énergie Atomique et aux Énergies Alternatives / CEA, France; the Bundesministerium für Bildung und Forschung, Deutsche Forschungsgemeinschaft, and Helmholtz-Gemeinschaft Deutscher Forschungszentren, Germany; the General Secretariat for Research and Technology, Greece; the National Scientific Research Foundation, and National Office for Research and Technology, Hungary; the Department of Atomic Energy and the Department of Science and Technology, India; the Institute for Studies in Theoretical Physics and Mathematics, Iran; the Science Foundation, Ireland; the Istituto Nazionale di Fisica Nucleare, Italy; the Korean Ministry of Education, Science and Technology and the World Class University program of NRF, Korea; the Lithuanian Academy of Sciences; the Mexican Funding Agencies (CINVESTAV, CONACYT, SEP, and UASLP-FAI); the Ministry of Science and Innovation, New Zealand; the Pakistan Atomic Energy Commission; the State Commission for Scientific Research, Poland; the Fundação para a Ciência e a Tecnologia, Portugal; JINR (Armenia, Belarus, Georgia, Ukraine, Uzbekistan); the Ministry of Science and Technologies of the Russian Federation, the Russian Ministry of Atomic Energy and the Russian Foundation for Basic Research; the Ministry of Science and Technological Development of Serbia; the Ministerio de Ciencia e Innovación, and Programa Consolider-Ingenio 2010, Spain; the Swiss Funding Agencies (ETH Board, ETH Zurich, PSI, SNF, UniZH, Canton Zurich, and SER); the National Science Council, Taipei; the Scientific and Technical Research Council of Turkey, and Turkish Atomic Energy Authority; the Science and Technology Facilities Council, UK; the US Department of Energy, and the US National Science Foundation.

Individuals have received support from the Marie-Curie programme and the European Research Council (European Union); the Leventis Foundation; the A. P. Sloan Foundation; the Alexander von Humboldt Foundation; the Belgian Federal Science Policy Office; the Fonds pour la Formation à la Recherche dans l'Industrie et dans l'Agriculture (FRIA-Belgium); the Agentschap voor Innovatie door Wetenschap en Technologie (IWT-Belgium); and the Council of Science and Industrial Research, India.

References

[1] C. Anastasiou, L. Dixon, and F. Petriello, "High precision QCD at hadron colliders: Electroweak gauge boson rapidity distributions at NNLO", *Phys. Rev. D* **69** (2004) 094008. doi:10.1103/PhysRevD.69.094008.

[2] K. Melnikov and F. Petriello, "Electroweak gauge boson production at hadron colliders through $O(\alpha_s^2)$", *Phys. Rev. D* **74** (2006) 114017. doi:10.1103/PhysRevD.74.114017.

[3] CMS Collaboration, "Measurement of the Inclusive W and Z Production Cross Sections in pp Collisions at $\sqrt{s}$ = 7 TeV", (2011). arXiv:1107.4789. Submitted to JHEP.

[4] CMS Collaboration, "Measurement of the Drell-Yan Cross Section in pp Collisions at $\sqrt{s}$ = 7 TeV", *JHEP* **10** (2011) 007. doi:10.1007/JHEP10(2011)007.

[5] D0 Collaboration, "Measurement of the shape of the boson transverse momentum distribution for $p\bar{p} \to Z/\gamma^* \to e^+e^- + X$ events produced at $\sqrt{s}$ of 1.96 TeV", *Phys. Rev. Lett.* **100** (2008) 102002. doi:10.1103/PhysRevLett.100.102002.

[6] D0 Collaboration, "Measurement of the normalized $Z/\gamma^* \to \mu^+\mu^-$ transverse momentum distribution in $p\bar{p}$ collisions at $\sqrt{s} = 1.96$ TeV", *Phys. Lett. B* **693** (2010) 522. doi:10.1016/j.physletb.2010.09.012.

[7] CDF Collaboration, "Measurement of $d\sigma/dy$ of Drell-Yan e^+e^- pairs in the Z mass region from $p\bar{p}$ collisions at $\sqrt{s}$ of 1.96 TeV", *Phys. Lett. B* **692** (2010) 232. doi:10.1016/j.physletb.2010.06.043.

[8] D0 Collaboration, "Measurement of the shape of the boson rapidity distribution for $p\bar{p} \to Z/\gamma^* \to e^+e^- + X$ events produced at $\sqrt{s}$ of 1.96 TeV", *Phys. Rev. D* **76** (2007) 012003. doi:10.1103/PhysRevD.76.012003.

[9] ATLAS Collaboration, "Measurement of the transverse momentum distribution of Z/γ^* bosons in proton-proton collisions at $\sqrt{s}$=7 TeV with the ATLAS detector", (2011). arXiv:1107.2381. Submitted to Physics Letters B.

[10] ATLAS Collaboration, "Measurement of the inclusive $W^\pm$ and Z/γ^* cross sections in the e and μ decay channels in pp collisions at $\sqrt{s} = 7$ TeV with the ATLAS detector", (2011). arXiv:1109.5141. Submitted to Physical Review D.

[11] CMS Collaboration, "The CMS experiment at the CERN LHC", *JINST* **3** (2008) S08004. doi:10.1088/1748-0221/3/08/S08004.

[12] CMS Collaboration, "Measurements of inclusive W and Z cross sections in pp collisions at $\sqrt{s}$=7 TeV", *JHEP* **11** (2011) 1. doi:10.1007/JHEP01(2011)080.

[13] S. Frixione, P. Nason, and C. Oleari, "Matching NLO QCD computations with Parton Shower simulations: the POWHEG method", *JHEP* **11** (2007) 070, arXiv:0709.2092. doi:10.1088/1126-6708/2007/11/070.

[14] T. Sjöstrand, S. Mrenna, and P. Skands, "PYTHIA 6.4 Physics and Manual", *JHEP* **05** (2006) 026. doi:10.1088/1126-6708/2006/05/026.

[15] H.-L. Lai, M. Guzzi, J. Huston et al., "New parton distributions for collider physics", *Phys. Rev. D* **82** (2010) 074024. doi:10.1103/PhysRevD.82.074024.

[16] R. Field, "Early LHC Underlying Event Data - Findings and Surprises", (2010). arXiv:1010.3558.

[17] CMS Collaboration, "Measurement of the underlying event activity at the LHC with $\sqrt{s} = 7$ TeV and comparison with $\sqrt{s} = 0.9$ TeV", *Journal of High Energy Physics* **2011** (2011) 1–31. doi:10.1007/JHEP09(2011)109.

[18] GEANT4 Collaboration, "GEANT4– a simulation toolkit", *Nucl. Instrum. Meth. A* **506** (2003) 250. doi:10.1016/S0168-9002(03)01368-8.

[19] F. Maltoni and T. Stelzer, "MadEvent: automatic event generation with MadGraph", *JHEP* **02** (2003) 027. doi:10.1088/1126-6708/2003/02/027.

[20] V. Blobel, "An Unfolding method for high-energy physics experiments", (2002). arXiv:hep-ex/0208022.

[21] A. Valassi, "Combining correlated measurements of several different physical quantities", *Nucl. Instrum. Meth. A* **500** (2003) 391. doi:10.1016/S0168-9002(03)00329-2.

[22] A. Martin, W. Stirling, R. Thorne et al., "Parton distributions for the LHC", *Eur. Phys. J. C* **63** (2009) 189. doi:10.1140/epjc/s10052-009-1072-5.

[23] H1 and ZEUS Collaborations, "HERA Precision Measurements and Impact for LHC Predictions", (2011). arXiv:1107.4193.

[24] NNPDF Collaboration, "A first unbiased global NLO determination of parton distributions and their uncertainties", *Nucl. Phys. B* **838** (2010) 136. doi:10.1016/j.nuclphysb.2010.05.008.

[25] P. Z. Skands, "Tuning Monte Carlo Generators: The Perugia Tunes", *Phys. Rev. D* **82** (2010) 074018. doi:10.1103/PhysRevD.82.074018.

[26] A. Buckley, H. Hoeth, H. Lacker et al., "Systematic event generator tuning for the LHC", *Eur. Phys. J. C* **65** (2010) 331. doi:10.1140/epjc/s10052-009-1196-7.

[27] R. Gavin, Y. Li, F. Petriello et al., "FEWZ 2.0: A code for hadronic Z production at next-to-next-to-leading order", *Comput. Phys. Commun.* **182** (2011) 2388. doi:10.1016/j.cpc.2011.06.008.

A The CMS Collaboration

Yerevan Physics Institute, Yerevan, Armenia
S. Chatrchyan, V. Khachatryan, A.M. Sirunyan, A. Tumasyan

Institut für Hochenergiephysik der OeAW, Wien, Austria
W. Adam, T. Bergauer, M. Dragicevic, J. Erö, C. Fabjan, M. Friedl, R. Frühwirth, V.M. Ghete, J. Hammer[1], M. Hoch, N. Hörmann, J. Hrubec, M. Jeitler, W. Kiesenhofer, M. Krammer, D. Liko, I. Mikulec, M. Pernicka, B. Rahbaran, H. Rohringer, R. Schöfbeck, J. Strauss, A. Taurok, F. Teischinger, C. Trauner, P. Wagner, W. Waltenberger, G. Walzel, E. Widl, C.-E. Wulz

National Centre for Particle and High Energy Physics, Minsk, Belarus
V. Mossolov, N. Shumeiko, J. Suarez Gonzalez

Universiteit Antwerpen, Antwerpen, Belgium
S. Bansal, L. Benucci, E.A. De Wolf, X. Janssen, S. Luyckx, T. Maes, L. Mucibello, S. Ochesanu, B. Roland, R. Rougny, M. Selvaggi, H. Van Haevermaet, P. Van Mechelen, N. Van Remortel

Vrije Universiteit Brussel, Brussel, Belgium
F. Blekman, S. Blyweert, J. D'Hondt, R. Gonzalez Suarez, A. Kalogeropoulos, M. Maes, A. Olbrechts, W. Van Doninck, P. Van Mulders, G.P. Van Onsem, I. Villella

Université Libre de Bruxelles, Bruxelles, Belgium
O. Charaf, B. Clerbaux, G. De Lentdecker, V. Dero, A.P.R. Gay, G.H. Hammad, T. Hreus, A. Léonard, P.E. Marage, L. Thomas, C. Vander Velde, P. Vanlaer

Ghent University, Ghent, Belgium
V. Adler, K. Beernaert, A. Cimmino, S. Costantini, M. Grunewald, B. Klein, J. Lellouch, A. Marinov, J. Mccartin, D. Ryckbosch, N. Strobbe, F. Thyssen, M. Tytgat, L. Vanelderen, P. Verwilligen, S. Walsh, N. Zaganidis

Université Catholique de Louvain, Louvain-la-Neuve, Belgium
S. Basegmez, G. Bruno, J. Caudron, L. Ceard, E. Cortina Gil, J. De Favereau De Jeneret, C. Delaere, D. Favart, L. Forthomme, A. Giammanco[2], G. Grégoire, J. Hollar, V. Lemaitre, J. Liao, O. Militaru, C. Nuttens, S. Ovyn, D. Pagano, A. Pin, K. Piotrzkowski, N. Schul

Université de Mons, Mons, Belgium
N. Beliy, T. Caebergs, E. Daubie

Centro Brasileiro de Pesquisas Fisicas, Rio de Janeiro, Brazil
G.A. Alves, D. De Jesus Damiao, M.E. Pol, M.H.G. Souza

Universidade do Estado do Rio de Janeiro, Rio de Janeiro, Brazil
W.L. Aldá Júnior, W. Carvalho, A. Custódio, E.M. Da Costa, C. De Oliveira Martins, S. Fonseca De Souza, D. Matos Figueiredo, L. Mundim, H. Nogima, V. Oguri, W.L. Prado Da Silva, A. Santoro, S.M. Silva Do Amaral, A. Sznajder

Instituto de Fisica Teorica, Universidade Estadual Paulista, Sao Paulo, Brazil
T.S. Anjos[3], C.A. Bernardes[3], F.A. Dias[4], T.R. Fernandez Perez Tomei, E. M. Gregores[3], C. Lagana, F. Marinho, P.G. Mercadante[3], S.F. Novaes, Sandra S. Padula

Institute for Nuclear Research and Nuclear Energy, Sofia, Bulgaria
N. Darmenov[1], V. Genchev[1], P. Iaydjiev[1], S. Piperov, M. Rodozov, S. Stoykova, G. Sultanov, V. Tcholakov, R. Trayanov, M. Vutova

University of Sofia, Sofia, Bulgaria
A. Dimitrov, R. Hadjiiska, A. Karadzhinova, V. Kozhuharov, L. Litov, M. Mateev, B. Pavlov, P. Petkov

Institute of High Energy Physics, Beijing, China
J.G. Bian, G.M. Chen, H.S. Chen, C.H. Jiang, D. Liang, S. Liang, X. Meng, J. Tao, J. Wang, J. Wang, X. Wang, Z. Wang, H. Xiao, M. Xu, J. Zang, Z. Zhang

State Key Lab. of Nucl. Phys. and Tech., Peking University, Beijing, China
Y. Ban, S. Guo, Y. Guo, W. Li, Y. Mao, S.J. Qian, H. Teng, B. Zhu, W. Zou

Universidad de Los Andes, Bogota, Colombia
A. Cabrera, B. Gomez Moreno, A.A. Ocampo Rios, A.F. Osorio Oliveros, J.C. Sanabria

Technical University of Split, Split, Croatia
N. Godinovic, D. Lelas, R. Plestina[5], D. Polic, I. Puljak

University of Split, Split, Croatia
Z. Antunovic, M. Dzelalija, M. Kovac

Institute Rudjer Boskovic, Zagreb, Croatia
V. Brigljevic, S. Duric, K. Kadija, J. Luetic, S. Morovic

University of Cyprus, Nicosia, Cyprus
A. Attikis, M. Galanti, J. Mousa, C. Nicolaou, F. Ptochos, P.A. Razis

Charles University, Prague, Czech Republic
M. Finger, M. Finger Jr.

Academy of Scientific Research and Technology of the Arab Republic of Egypt, Egyptian Network of High Energy Physics, Cairo, Egypt
Y. Assran[6], A. Ellithi Kamel[7], S. Khalil[8], M.A. Mahmoud[9], A. Radi[10]

National Institute of Chemical Physics and Biophysics, Tallinn, Estonia
A. Hektor, M. Kadastik, M. Müntel, M. Raidal, L. Rebane, A. Tiko

Department of Physics, University of Helsinki, Helsinki, Finland
V. Azzolini, P. Eerola, G. Fedi, M. Voutilainen

Helsinki Institute of Physics, Helsinki, Finland
S. Czellar, J. Härkönen, A. Heikkinen, V. Karimäki, R. Kinnunen, M.J. Kortelainen, T. Lampén, K. Lassila-Perini, S. Lehti, T. Lindén, P. Luukka, T. Mäenpää, E. Tuominen, J. Tuominiemi, E. Tuovinen, D. Ungaro, L. Wendland

Lappeenranta University of Technology, Lappeenranta, Finland
K. Banzuzi, A. Karjalainen, A. Korpela, T. Tuuva

Laboratoire d'Annecy-le-Vieux de Physique des Particules, IN2P3-CNRS, Annecy-le-Vieux, France
D. Sillou

DSM/IRFU, CEA/Saclay, Gif-sur-Yvette, France
M. Besancon, S. Choudhury, M. Dejardin, D. Denegri, B. Fabbro, J.L. Faure, F. Ferri, S. Ganjour, A. Givernaud, P. Gras, G. Hamel de Monchenault, P. Jarry, E. Locci, J. Malcles, M. Marionneau, L. Millischer, J. Rander, A. Rosowsky, I. Shreyber, M. Titov

Laboratoire Leprince-Ringuet, Ecole Polytechnique, IN2P3-CNRS, Palaiseau, France
S. Baffioni, F. Beaudette, L. Benhabib, L. Bianchini, M. Bluj[11], C. Broutin, P. Busson, C. Charlot, T. Dahms, L. Dobrzynski, S. Elgammal, R. Granier de Cassagnac, M. Haguenauer, P. Miné, C. Mironov, C. Ochando, P. Paganini, D. Sabes, R. Salerno, Y. Sirois, C. Thiebaux, C. Veelken, A. Zabi

Institut Pluridisciplinaire Hubert Curien, Université de Strasbourg, Université de Haute Alsace Mulhouse, CNRS/IN2P3, Strasbourg, France
J.-L. Agram[12], J. Andrea, D. Bloch, D. Bodin, J.-M. Brom, M. Cardaci, E.C. Chabert, C. Collard, E. Conte[12], F. Drouhin[12], C. Ferro, J.-C. Fontaine[12], D. Gelé, U. Goerlach, S. Greder, P. Juillot, M. Karim[12], A.-C. Le Bihan, P. Van Hove

Centre de Calcul de l'Institut National de Physique Nucleaire et de Physique des Particules (IN2P3), Villeurbanne, France
F. Fassi, D. Mercier

Université de Lyon, Université Claude Bernard Lyon 1, CNRS-IN2P3, Institut de Physique Nucléaire de Lyon, Villeurbanne, France
C. Baty, S. Beauceron, N. Beaupere, M. Bedjidian, O. Bondu, G. Boudoul, D. Boumediene, H. Brun, J. Chasserat, R. Chierici, D. Contardo, P. Depasse, H. El Mamouni, A. Falkiewicz, J. Fay, S. Gascon, B. Ille, T. Kurca, T. Le Grand, M. Lethuillier, L. Mirabito, S. Perries, V. Sordini, S. Tosi, Y. Tschudi, P. Verdier, S. Viret

Institute of High Energy Physics and Informatization, Tbilisi State University, Tbilisi, Georgia
D. Lomidze

RWTH Aachen University, I. Physikalisches Institut, Aachen, Germany
G. Anagnostou, S. Beranek, M. Edelhoff, L. Feld, N. Heracleous, O. Hindrichs, R. Jussen, K. Klein, J. Merz, A. Ostapchuk, A. Perieanu, F. Raupach, J. Sammet, S. Schael, D. Sprenger, H. Weber, M. Weber, B. Wittmer, V. Zhukov[13]

RWTH Aachen University, III. Physikalisches Institut A, Aachen, Germany
M. Ata, E. Dietz-Laursonn, M. Erdmann, T. Hebbeker, C. Heidemann, A. Hinzmann, K. Hoepfner, T. Klimkovich, D. Klingebiel, P. Kreuzer, D. Lanske†, J. Lingemann, C. Magass, M. Merschmeyer, A. Meyer, P. Papacz, H. Pieta, H. Reithler, S.A. Schmitz, L. Sonnenschein, J. Steggemann, D. Teyssier

RWTH Aachen University, III. Physikalisches Institut B, Aachen, Germany
M. Bontenackels, V. Cherepanov, M. Davids, G. Flügge, H. Geenen, M. Giffels, W. Haj Ahmad, F. Hoehle, B. Kargoll, T. Kress, Y. Kuessel, A. Linn, A. Nowack, L. Perchalla, O. Pooth, J. Rennefeld, P. Sauerland, A. Stahl, D. Tornier, M.H. Zoeller

Deutsches Elektronen-Synchrotron, Hamburg, Germany
M. Aldaya Martin, W. Behrenhoff, U. Behrens, M. Bergholz[14], A. Bethani, K. Borras, A. Cakir, A. Campbell, E. Castro, D. Dammann, G. Eckerlin, D. Eckstein, A. Flossdorf, G. Flucke, A. Geiser, J. Hauk, H. Jung[1], M. Kasemann, P. Katsas, C. Kleinwort, H. Kluge, A. Knutsson, M. Krämer, D. Krücker, E. Kuznetsova, W. Lange, W. Lohmann[14], B. Lutz, R. Mankel, I. Marfin, M. Marienfeld, I.-A. Melzer-Pellmann, A.B. Meyer, J. Mnich, A. Mussgiller, S. Naumann-Emme, J. Olzem, A. Petrukhin, D. Pitzl, A. Raspereza, M. Rosin, R. Schmidt[14], T. Schoerner-Sadenius, N. Sen, A. Spiridonov, M. Stein, J. Tomaszewska, R. Walsh, C. Wissing

University of Hamburg, Hamburg, Germany
C. Autermann, V. Blobel, S. Bobrovskyi, J. Draeger, H. Enderle, U. Gebbert, M. Görner,

T. Hermanns, K. Kaschube, G. Kaussen, H. Kirschenmann, R. Klanner, J. Lange, B. Mura, F. Nowak, N. Pietsch, C. Sander, H. Schettler, P. Schleper, E. Schlieckau, M. Schröder, T. Schum, H. Stadie, G. Steinbrück, J. Thomsen

Institut für Experimentelle Kernphysik, Karlsruhe, Germany
C. Barth, J. Bauer, J. Berger, V. Buege, T. Chwalek, W. De Boer, A. Dierlamm, G. Dirkes, M. Feindt, J. Gruschke, M. Guthoff[1], C. Hackstein, F. Hartmann, M. Heinrich, H. Held, K.H. Hoffmann, S. Honc, I. Katkov[13], J.R. Komaragiri, T. Kuhr, D. Martschei, S. Mueller, Th. Müller, M. Niegel, O. Oberst, A. Oehler, J. Ott, T. Peiffer, G. Quast, K. Rabbertz, F. Ratnikov, N. Ratnikova, M. Renz, S. Röcker, C. Saout, A. Scheurer, P. Schieferdecker, F.-P. Schilling, M. Schmanau, G. Schott, H.J. Simonis, F.M. Stober, D. Troendle, J. Wagner-Kuhr, T. Weiler, M. Zeise, E.B. Ziebarth

Institute of Nuclear Physics "Demokritos", Aghia Paraskevi, Greece
G. Daskalakis, T. Geralis, S. Kesisoglou, A. Kyriakis, D. Loukas, I. Manolakos, A. Markou, C. Markou, C. Mavrommatis, E. Ntomari, E. Petrakou

University of Athens, Athens, Greece
L. Gouskos, T.J. Mertzimekis, A. Panagiotou, N. Saoulidou, E. Stiliaris

University of Ioánnina, Ioánnina, Greece
I. Evangelou, C. Foudas[1], P. Kokkas, N. Manthos, I. Papadopoulos, V. Patras, F.A. Triantis

KFKI Research Institute for Particle and Nuclear Physics, Budapest, Hungary
A. Aranyi, G. Bencze, L. Boldizsar, C. Hajdu[1], P. Hidas, D. Horvath[15], A. Kapusi, K. Krajczar[16], F. Sikler[1], G.I. Veres[16], G. Vesztergombi[16]

Institute of Nuclear Research ATOMKI, Debrecen, Hungary
N. Beni, J. Molnar, J. Palinkas, Z. Szillasi, V. Veszpremi

University of Debrecen, Debrecen, Hungary
J. Karancsi, P. Raics, Z.L. Trocsanyi, B. Ujvari

Panjab University, Chandigarh, India
S.B. Beri, V. Bhatnagar, N. Dhingra, R. Gupta, M. Jindal, M. Kaur, J.M. Kohli, M.Z. Mehta, N. Nishu, L.K. Saini, A. Sharma, A.P. Singh, J. Singh, S.P. Singh

University of Delhi, Delhi, India
S. Ahuja, B.C. Choudhary, P. Gupta, A. Kumar, A. Kumar, S. Malhotra, M. Naimuddin, K. Ranjan, R.K. Shivpuri

Saha Institute of Nuclear Physics, Kolkata, India
S. Banerjee, S. Bhattacharya, S. Dutta, B. Gomber, S. Jain, S. Jain, R. Khurana, S. Sarkar

Bhabha Atomic Research Centre, Mumbai, India
R.K. Choudhury, D. Dutta, S. Kailas, V. Kumar, A.K. Mohanty[1], L.M. Pant, P. Shukla

Tata Institute of Fundamental Research - EHEP, Mumbai, India
T. Aziz, M. Guchait[17], A. Gurtu, M. Maity[18], D. Majumder, G. Majumder, K. Mazumdar, G.B. Mohanty, B. Parida, A. Saha, K. Sudhakar, N. Wickramage

Tata Institute of Fundamental Research - HECR, Mumbai, India
S. Banerjee, S. Dugad, N.K. Mondal

Institute for Research and Fundamental Sciences (IPM), Tehran, Iran
H. Arfaei, H. Bakhshiansohi[19], S.M. Etesami[20], A. Fahim[19], M. Hashemi, H. Hesari, A. Jafari[19],

M. Khakzad, A. Mohammadi[21], M. Mohammadi Najafabadi, S. Paktinat Mehdiabadi, B. Safarzadeh, M. Zeinali[20]

INFN Sezione di Bari [a], Università di Bari [b], Politecnico di Bari [c], Bari, Italy
M. Abbrescia[a,b], L. Barbone[a,b], C. Calabria[a,b], A. Colaleo[a], D. Creanza[a,c], N. De Filippis[a,c,1], M. De Palma[a,b], L. Fiore[a], G. Iaselli[a,c], L. Lusito[a,b], G. Maggi[a,c], M. Maggi[a], N. Manna[a,b], B. Marangelli[a,b], S. My[a,c], S. Nuzzo[a,b], N. Pacifico[a,b], A. Pompili[a,b], G. Pugliese[a,c], F. Romano[a,c], G. Selvaggi[a,b], L. Silvestris[a], S. Tupputi[a,b], G. Zito[a]

INFN Sezione di Bologna [a], Università di Bologna [b], Bologna, Italy
G. Abbiendi[a], A.C. Benvenuti[a], D. Bonacorsi[a], S. Braibant-Giacomelli[a,b], L. Brigliadori[a], P. Capiluppi[a,b], A. Castro[a,b], F.R. Cavallo[a], M. Cuffiani[a,b], G.M. Dallavalle[a], F. Fabbri[a], A. Fanfani[a,b], D. Fasanella[a,1], P. Giacomelli[a], M. Giunta[a], C. Grandi[a], S. Marcellini[a], G. Masetti[a], M. Meneghelli[a,b], A. Montanari[a], F.L. Navarria[a,b], F. Odorici[a], A. Perrotta[a], F. Primavera[a], A.M. Rossi[a,b], T. Rovelli[a,b], G. Siroli[a,b], R. Travaglini[a,b]

INFN Sezione di Catania [a], Università di Catania [b], Catania, Italy
S. Albergo[a,b], G. Cappello[a,b], M. Chiorboli[a,b], S. Costa[a,b], R. Potenza[a,b], A. Tricomi[a,b], C. Tuve[a,b]

INFN Sezione di Firenze [a], Università di Firenze [b], Firenze, Italy
G. Barbagli[a], V. Ciulli[a,b], C. Civinini[a], R. D'Alessandro[a,b], E. Focardi[a,b], S. Frosali[a,b], E. Gallo[a], S. Gonzi[a,b], M. Meschini[a], S. Paoletti[a], G. Sguazzoni[a], A. Tropiano[a,1]

INFN Laboratori Nazionali di Frascati, Frascati, Italy
L. Benussi, S. Bianco, S. Colafranceschi[22], F. Fabbri, D. Piccolo

INFN Sezione di Genova, Genova, Italy
P. Fabbricatore, R. Musenich

INFN Sezione di Milano-Bicocca [a], Università di Milano-Bicocca [b], Milano, Italy
A. Benaglia[a,b,1], F. De Guio[a,b], L. Di Matteo[a,b], S. Gennai[a,1], A. Ghezzi[a,b], S. Malvezzi[a], A. Martelli[a,b], A. Massironi[a,b,1], D. Menasce[a], L. Moroni[a], M. Paganoni[a,b], D. Pedrini[a], S. Ragazzi[a,b], N. Redaelli[a], S. Sala[a], T. Tabarelli de Fatis[a,b]

INFN Sezione di Napoli [a], Università di Napoli "Federico II" [b], Napoli, Italy
S. Buontempo[a], C.A. Carrillo Montoya[a,1], N. Cavallo[a,23], A. De Cosa[a,b], O. Dogangun[a,b], F. Fabozzi[a,23], A.O.M. Iorio[a,1], L. Lista[a], M. Merola[a,b], P. Paolucci[a]

INFN Sezione di Padova [a], Università di Padova [b], Università di Trento (Trento) [c], Padova, Italy
P. Azzi[a], N. Bacchetta[a,1], P. Bellan[a,b], D. Bisello[a,b], A. Branca[a], R. Carlin[a,b], P. Checchia[a], T. Dorigo[a], U. Dosselli[a], F. Fanzago[a], F. Gasparini[a,b], U. Gasparini[a,b], A. Gozzelino[a], S. Lacaprara[a,24], I. Lazzizzera[a,c], M. Margoni[a,b], M. Mazzucato[a], A.T. Meneguzzo[a,b], M. Nespolo[a,1], L. Perrozzi[a], N. Pozzobon[a,b], P. Ronchese[a,b], F. Simonetto[a,b], E. Torassa[a], M. Tosi[a,b,1], S. Vanini[a,b], P. Zotto[a,b], G. Zumerle[a,b]

INFN Sezione di Pavia [a], Università di Pavia [b], Pavia, Italy
P. Baesso[a,b], U. Berzano[a], S.P. Ratti[a,b], C. Riccardi[a,b], P. Torre[a,b], P. Vitulo[a,b], C. Viviani[a,b]

INFN Sezione di Perugia [a], Università di Perugia [b], Perugia, Italy
M. Biasini[a,b], G.M. Bilei[a], B. Caponeri[a,b], L. Fanò[a,b], P. Lariccia[a,b], A. Lucaroni[a,b,1], G. Mantovani[a,b], M. Menichelli[a], A. Nappi[a,b], F. Romeo[a,b], A. Santocchia[a,b], S. Taroni[a,b,1], M. Valdata[a,b]

INFN Sezione di Pisa [a], Università di Pisa [b], Scuola Normale Superiore di Pisa [c], Pisa, Italy
P. Azzurri[a,c], G. Bagliesi[a], J. Bernardini[a,b], T. Boccali[a], G. Broccolo[a,c], R. Castaldi[a], R.T. D'Agnolo[a,c], R. Dell'Orso[a], F. Fiori[a,b], L. Foà[a,c], A. Giassi[a], A. Kraan[a], F. Ligabue[a,c], T. Lomtadze[a], L. Martini[a,25], A. Messineo[a,b], F. Palla[a], F. Palmonari[a], A. Rizzi, G. Segneri[a], A.T. Serban[a], P. Spagnolo[a], R. Tenchini[a], G. Tonelli[a,b,1], A. Venturi[a,1], P.G. Verdini[a]

INFN Sezione di Roma [a], Università di Roma "La Sapienza" [b], Roma, Italy
L. Barone[a,b], F. Cavallari[a], D. Del Re[a,b,1], M. Diemoz[a], D. Franci[a,b], M. Grassi[a,1], E. Longo[a,b], P. Meridiani[a], S. Nourbakhsh[a], G. Organtini[a,b], F. Pandolfi[a,b], R. Paramatti[a], S. Rahatlou[a,b], M. Sigamani[a]

INFN Sezione di Torino [a], Università di Torino [b], Università del Piemonte Orientale (Novara) [c], Torino, Italy
N. Amapane[a,b], R. Arcidiacono[a,c], S. Argiro[a,b], M. Arneodo[a,c], C. Biino[a], C. Botta[a,b], N. Cartiglia[a], R. Castello[a,b], M. Costa[a,b], N. Demaria[a], A. Graziano[a,b], C. Mariotti[a], S. Maselli[a], E. Migliore[a,b], V. Monaco[a,b], M. Musich[a], M.M. Obertino[a,c], N. Pastrone[a], M. Pelliccioni[a], A. Potenza[a,b], A. Romero[a,b], M. Ruspa[a,c], R. Sacchi[a,b], V. Sola[a,b], A. Solano[a,b], A. Staiano[a], A. Vilela Pereira[a]

INFN Sezione di Trieste [a], Università di Trieste [b], Trieste, Italy
S. Belforte[a], F. Cossutti[a], G. Della Ricca[a,b], B. Gobbo[a], M. Marone[a,b], D. Montanino[a,b,1], A. Penzo[a]

Kangwon National University, Chunchon, Korea
S.G. Heo, S.K. Nam

Kyungpook National University, Daegu, Korea
S. Chang, J. Chung, D.H. Kim, G.N. Kim, J.E. Kim, D.J. Kong, H. Park, S.R. Ro, D.C. Son, T. Son

Chonnam National University, Institute for Universe and Elementary Particles, Kwangju, Korea
J.Y. Kim, Zero J. Kim, S. Song

Konkuk University, Seoul, Korea
H.Y. Jo

Korea University, Seoul, Korea
S. Choi, D. Gyun, B. Hong, M. Jo, H. Kim, T.J. Kim, K.S. Lee, D.H. Moon, S.K. Park, E. Seo, K.S. Sim

University of Seoul, Seoul, Korea
M. Choi, S. Kang, H. Kim, J.H. Kim, C. Park, I.C. Park, S. Park, G. Ryu

Sungkyunkwan University, Suwon, Korea
Y. Cho, Y. Choi, Y.K. Choi, J. Goh, M.S. Kim, B. Lee, J. Lee, S. Lee, H. Seo, I. Yu

Vilnius University, Vilnius, Lithuania
M.J. Bilinskas, I. Grigelionis, M. Janulis, D. Martisiute, P. Petrov, M. Polujanskas, T. Sabonis

Centro de Investigacion y de Estudios Avanzados del IPN, Mexico City, Mexico
H. Castilla-Valdez, E. De La Cruz-Burelo, I. Heredia-de La Cruz, R. Lopez-Fernandez, R. Magaña Villalba, J. Martínez-Ortega, A. Sánchez-Hernández, L.M. Villasenor-Cendejas

Universidad Iberoamericana, Mexico City, Mexico
S. Carrillo Moreno, F. Vazquez Valencia

Benemerita Universidad Autonoma de Puebla, Puebla, Mexico
H.A. Salazar Ibarguen

Universidad Autónoma de San Luis Potosí, San Luis Potosí, Mexico
E. Casimiro Linares, A. Morelos Pineda, M.A. Reyes-Santos

University of Auckland, Auckland, New Zealand
D. Krofcheck, J. Tam

University of Canterbury, Christchurch, New Zealand
A.J. Bell, P.H. Butler, R. Doesburg, H. Silverwood, N. Tambe

National Centre for Physics, Quaid-I-Azam University, Islamabad, Pakistan
M. Ahmad, M.I. Asghar, H.R. Hoorani, S. Khalid, W.A. Khan, T. Khurshid, S. Qazi, M.A. Shah, M. Shoaib

Institute of Experimental Physics, Faculty of Physics, University of Warsaw, Warsaw, Poland
G. Brona, M. Cwiok, W. Dominik, K. Doroba, A. Kalinowski, M. Konecki, J. Krolikowski

Soltan Institute for Nuclear Studies, Warsaw, Poland
T. Frueboes, R. Gokieli, M. Górski, M. Kazana, K. Nawrocki, K. Romanowska-Rybinska, M. Szleper, G. Wrochna, P. Zalewski

Laboratório de Instrumentação e Física Experimental de Partículas, Lisboa, Portugal
N. Almeida, P. Bargassa, A. David, P. Faccioli, P.G. Ferreira Parracho, M. Gallinaro, P. Musella, A. Nayak, J. Pela[1], P.Q. Ribeiro, J. Seixas, J. Varela

Joint Institute for Nuclear Research, Dubna, Russia
S. Afanasiev, I. Belotelov, P. Bunin, M. Gavrilenko, I. Golutvin, I. Gorbunov, A. Kamenev, V. Karjavin, G. Kozlov, A. Lanev, P. Moisenz, V. Palichik, V. Perelygin, S. Shmatov, V. Smirnov, A. Volodko, A. Zarubin

Petersburg Nuclear Physics Institute, Gatchina (St Petersburg), Russia
S. Evstyukhin, V. Golovtsov, Y. Ivanov, V. Kim, P. Levchenko, V. Murzin, V. Oreshkin, I. Smirnov, V. Sulimov, L. Uvarov, S. Vavilov, A. Vorobyev, An. Vorobyev

Institute for Nuclear Research, Moscow, Russia
Yu. Andreev, A. Dermenev, S. Gninenko, N. Golubev, M. Kirsanov, N. Krasnikov, V. Matveev, A. Pashenkov, A. Toropin, S. Troitsky

Institute for Theoretical and Experimental Physics, Moscow, Russia
V. Epshteyn, M. Erofeeva, V. Gavrilov, V. Kaftanov†, M. Kossov[1], A. Krokhotin, N. Lychkovskaya, V. Popov, G. Safronov, S. Semenov, V. Stolin, E. Vlasov, A. Zhokin

Moscow State University, Moscow, Russia
A. Belyaev, E. Boos, M. Dubinin[4], L. Dudko, A. Ershov, A. Gribushin, O. Kodolova, I. Lokhtin, A. Markina, S. Obraztsov, M. Perfilov, S. Petrushanko, L. Sarycheva, V. Savrin, A. Snigirev

P.N. Lebedev Physical Institute, Moscow, Russia
V. Andreev, M. Azarkin, I. Dremin, M. Kirakosyan, A. Leonidov, G. Mesyats, S.V. Rusakov, A. Vinogradov

State Research Center of Russian Federation, Institute for High Energy Physics, Protvino, Russia
I. Azhgirey, I. Bayshev, S. Bitioukov, V. Grishin[1], V. Kachanov, D. Konstantinov, A. Korablev,

V. Krychkine, V. Petrov, R. Ryutin, A. Sobol, L. Tourtchanovitch, S. Troshin, N. Tyurin, A. Uzunian, A. Volkov

University of Belgrade, Faculty of Physics and Vinca Institute of Nuclear Sciences, Belgrade, Serbia
P. Adzic[26], M. Djordjevic, M. Ekmedzic, D. Krpic[26], J. Milosevic

Centro de Investigaciones Energéticas Medioambientales y Tecnológicas (CIEMAT), Madrid, Spain
M. Aguilar-Benitez, J. Alcaraz Maestre, P. Arce, C. Battilana, E. Calvo, M. Cerrada, M. Chamizo Llatas, N. Colino, B. De La Cruz, A. Delgado Peris, C. Diez Pardos, D. Domínguez Vázquez, C. Fernandez Bedoya, J.P. Fernández Ramos, A. Ferrando, J. Flix, M.C. Fouz, P. Garcia-Abia, O. Gonzalez Lopez, S. Goy Lopez, J.M. Hernandez, M.I. Josa, G. Merino, J. Puerta Pelayo, I. Redondo, L. Romero, J. Santaolalla, M.S. Soares, C. Willmott

Universidad Autónoma de Madrid, Madrid, Spain
C. Albajar, G. Codispoti, J.F. de Trocóniz

Universidad de Oviedo, Oviedo, Spain
J. Cuevas, J. Fernandez Menendez, S. Folgueras, I. Gonzalez Caballero, L. Lloret Iglesias, J.M. Vizan Garcia

Instituto de Física de Cantabria (IFCA), CSIC-Universidad de Cantabria, Santander, Spain
J.A. Brochero Cifuentes, I.J. Cabrillo, A. Calderon, S.H. Chuang, J. Duarte Campderros, M. Felcini[27], M. Fernandez, G. Gomez, J. Gonzalez Sanchez, C. Jorda, P. Lobelle Pardo, A. Lopez Virto, J. Marco, R. Marco, C. Martinez Rivero, F. Matorras, F.J. Munoz Sanchez, J. Piedra Gomez[28], T. Rodrigo, A.Y. Rodríguez-Marrero, A. Ruiz-Jimeno, L. Scodellaro, M. Sobron Sanudo, I. Vila, R. Vilar Cortabitarte

CERN, European Organization for Nuclear Research, Geneva, Switzerland
D. Abbaneo, E. Auffray, G. Auzinger, P. Baillon, A.H. Ball, D. Barney, C. Bernet[5], W. Bialas, P. Bloch, A. Bocci, M. Bona, H. Breuker, K. Bunkowski, T. Camporesi, G. Cerminara, T. Christiansen, J.A. Coarasa Perez, B. Curé, D. D'Enterria, A. De Roeck, S. Di Guida, N. Dupont-Sagorin, A. Elliott-Peisert, B. Frisch, W. Funk, A. Gaddi, G. Georgiou, H. Gerwig, D. Gigi, K. Gill, D. Giordano, F. Glege, R. Gomez-Reino Garrido, M. Gouzevitch, P. Govoni, S. Gowdy, R. Guida, L. Guiducci, S. Gundacker, M. Hansen, C. Hartl, J. Harvey, J. Hegeman, B. Hegner, H.F. Hoffmann, V. Innocente, P. Janot, K. Kaadze, E. Karavakis, P. Lecoq, P. Lenzi, C. Lourenço, T. Mäki, M. Malberti, L. Malgeri, M. Mannelli, L. Masetti, A. Maurisset, G. Mavromanolakis, F. Meijers, S. Mersi, E. Meschi, R. Moser, M.U. Mozer, M. Mulders, E. Nesvold, M. Nguyen, T. Orimoto, L. Orsini, E. Palencia Cortezon, E. Perez, A. Petrilli, A. Pfeiffer, M. Pierini, M. Pimiä, D. Piparo, G. Polese, L. Quertenmont, A. Racz, W. Reece, J. Rodrigues Antunes, G. Rolandi[29], T. Rommerskirchen, C. Rovelli[30], M. Rovere, H. Sakulin, F. Santanastasio, C. Schäfer, C. Schwick, I. Segoni, A. Sharma, P. Siegrist, P. Silva, M. Simon, P. Sphicas[31], D. Spiga, M. Spiropulu[4], M. Stoye, A. Tsirou, P. Vichoudis, H.K. Wöhri, S.D. Worm[32], W.D. Zeuner

Paul Scherrer Institut, Villigen, Switzerland
W. Bertl, K. Deiters, W. Erdmann, K. Gabathuler, R. Horisberger, Q. Ingram, H.C. Kaestli, S. König, D. Kotlinski, U. Langenegger, F. Meier, D. Renker, T. Rohe, J. Sibille[33]

Institute for Particle Physics, ETH Zurich, Zurich, Switzerland
L. Bäni, P. Bortignon, B. Casal, N. Chanon, Z. Chen, S. Cittolin, A. Deisher, G. Dissertori, M. Dittmar, J. Eugster, K. Freudenreich, C. Grab, P. Lecomte, W. Lustermann, C. Marchica[34],

P. Martinez Ruiz del Arbol, P. Milenovic[35], N. Mohr, F. Moortgat, C. Nägeli[34], P. Nef, F. Nessi-Tedaldi, L. Pape, F. Pauss, M. Peruzzi, F.J. Ronga, M. Rossini, L. Sala, A.K. Sanchez, M.-C. Sawley, A. Starodumov[36], B. Stieger, M. Takahashi, L. Tauscher†, A. Thea, K. Theofilatos, D. Treille, C. Urscheler, R. Wallny, M. Weber, L. Wehrli, J. Weng

Universität Zürich, Zurich, Switzerland
E. Aguilo, C. Amsler, V. Chiochia, S. De Visscher, C. Favaro, M. Ivova Rikova, B. Millan Mejias, P. Otiougova, P. Robmann, A. Schmidt, H. Snoek, M. Verzetti

National Central University, Chung-Li, Taiwan
Y.H. Chang, K.H. Chen, C.M. Kuo, S.W. Li, W. Lin, Z.K. Liu, Y.J. Lu, D. Mekterovic, R. Volpe, S.S. Yu

National Taiwan University (NTU), Taipei, Taiwan
P. Bartalini, P. Chang, Y.H. Chang, Y.W. Chang, Y. Chao, K.F. Chen, C. Dietz, U. Grundler, W.-S. Hou, Y. Hsiung, K.Y. Kao, Y.J. Lei, R.-S. Lu, J.G. Shiu, Y.M. Tzeng, X. Wan, M. Wang

Cukurova University, Adana, Turkey
A. Adiguzel, M.N. Bakirci[37], S. Cerci[38], C. Dozen, I. Dumanoglu, E. Eskut, S. Girgis, G. Gokbulut, I. Hos, E.E. Kangal, A. Kayis Topaksu, G. Onengut, K. Ozdemir, S. Ozturk[39], A. Polatoz, K. Sogut[40], D. Sunar Cerci[38], B. Tali[38], H. Topakli[37], D. Uzun, L.N. Vergili, M. Vergili

Middle East Technical University, Physics Department, Ankara, Turkey
I.V. Akin, T. Aliev, B. Bilin, S. Bilmis, M. Deniz, H. Gamsizkan, A.M. Guler, K. Ocalan, A. Ozpineci, M. Serin, R. Sever, U.E. Surat, M. Yalvac, E. Yildirim, M. Zeyrek

Bogazici University, Istanbul, Turkey
M. Deliomeroglu, E. Gülmez, B. Isildak, M. Kaya[41], O. Kaya[41], M. Özbek, S. Ozkorucuklu[42], N. Sonmez[43]

National Scientific Center, Kharkov Institute of Physics and Technology, Kharkov, Ukraine
L. Levchuk

University of Bristol, Bristol, United Kingdom
F. Bostock, J.J. Brooke, E. Clement, D. Cussans, R. Frazier, J. Goldstein, M. Grimes, G.P. Heath, H.F. Heath, L. Kreczko, S. Metson, D.M. Newbold[32], K. Nirunpong, A. Poll, S. Senkin, V.J. Smith

Rutherford Appleton Laboratory, Didcot, United Kingdom
L. Basso[44], K.W. Bell, A. Belyaev[44], C. Brew, R.M. Brown, B. Camanzi, D.J.A. Cockerill, J.A. Coughlan, K. Harder, S. Harper, J. Jackson, B.W. Kennedy, E. Olaiya, D. Petyt, B.C. Radburn-Smith, C.H. Shepherd-Themistocleous, I.R. Tomalin, W.J. Womersley

Imperial College, London, United Kingdom
R. Bainbridge, G. Ball, J. Ballin, R. Beuselinck, O. Buchmuller, D. Colling, N. Cripps, M. Cutajar, G. Davies, M. Della Negra, W. Ferguson, J. Fulcher, D. Futyan, A. Gilbert, A. Guneratne Bryer, G. Hall, Z. Hatherell, J. Hays, G. Iles, M. Jarvis, G. Karapostoli, L. Lyons, A.-M. Magnan, J. Marrouche, B. Mathias, R. Nandi, J. Nash, A. Nikitenko[36], A. Papageorgiou, M. Pesaresi, K. Petridis, M. Pioppi[45], D.M. Raymond, S. Rogerson, N. Rompotis, A. Rose, M.J. Ryan, C. Seez, P. Sharp, A. Sparrow, A. Tapper, S. Tourneur, M. Vazquez Acosta, T. Virdee, S. Wakefield, N. Wardle, D. Wardrope, T. Whyntie

Brunel University, Uxbridge, United Kingdom
M. Barrett, M. Chadwick, J.E. Cole, P.R. Hobson, A. Khan, P. Kyberd, D. Leslie, W. Martin, I.D. Reid, L. Teodorescu

Baylor University, Waco, USA
K. Hatakeyama, H. Liu

The University of Alabama, Tuscaloosa, USA
C. Henderson

Boston University, Boston, USA
A. Avetisyan, T. Bose, E. Carrera Jarrin, C. Fantasia, A. Heister, J. St. John, P. Lawson, D. Lazic, J. Rohlf, D. Sperka, L. Sulak

Brown University, Providence, USA
S. Bhattacharya, D. Cutts, A. Ferapontov, U. Heintz, S. Jabeen, G. Kukartsev, G. Landsberg, M. Luk, M. Narain, D. Nguyen, M. Segala, T. Sinthuprasith, T. Speer, K.V. Tsang

University of California, Davis, Davis, USA
R. Breedon, G. Breto, M. Calderon De La Barca Sanchez, S. Chauhan, M. Chertok, J. Conway, R. Conway, P.T. Cox, J. Dolen, R. Erbacher, R. Houtz, W. Ko, A. Kopecky, R. Lander, H. Liu, O. Mall, S. Maruyama, T. Miceli, D. Pellett, J. Robles, B. Rutherford, M. Searle, J. Smith, M. Squires, M. Tripathi, R. Vasquez Sierra

University of California, Los Angeles, Los Angeles, USA
V. Andreev, K. Arisaka, D. Cline, R. Cousins, J. Duris, S. Erhan, P. Everaerts, C. Farrell, J. Hauser, M. Ignatenko, C. Jarvis, C. Plager, G. Rakness, P. Schlein†, J. Tucker, V. Valuev

University of California, Riverside, Riverside, USA
J. Babb, R. Clare, J. Ellison, J.W. Gary, F. Giordano, G. Hanson, G.Y. Jeng, S.C. Kao, H. Liu, O.R. Long, A. Luthra, H. Nguyen, S. Paramesvaran, J. Sturdy, S. Sumowidagdo, R. Wilken, S. Wimpenny

University of California, San Diego, La Jolla, USA
W. Andrews, J.G. Branson, G.B. Cerati, D. Evans, F. Golf, A. Holzner, M. Lebourgeois, J. Letts, B. Mangano, S. Padhi, C. Palmer, G. Petrucciani, H. Pi, M. Pieri, R. Ranieri, M. Sani, V. Sharma, S. Simon, E. Sudano, M. Tadel, Y. Tu, A. Vartak, S. Wasserbaech[46], F. Würthwein, A. Yagil, J. Yoo

University of California, Santa Barbara, Santa Barbara, USA
D. Barge, R. Bellan, C. Campagnari, M. D'Alfonso, T. Danielson, K. Flowers, P. Geffert, C. George, J. Incandela, C. Justus, P. Kalavase, S.A. Koay, D. Kovalskyi[1], V. Krutelyov, S. Lowette, N. Mccoll, S.D. Mullin, V. Pavlunin, F. Rebassoo, J. Ribnik, J. Richman, R. Rossin, D. Stuart, W. To, J.R. Vlimant, C. West

California Institute of Technology, Pasadena, USA
A. Apresyan, A. Bornheim, J. Bunn, Y. Chen, E. Di Marco, J. Duarte, M. Gataullin, Y. Ma, A. Mott, H.B. Newman, C. Rogan, V. Timciuc, P. Traczyk, J. Veverka, R. Wilkinson, Y. Yang, R.Y. Zhu

Carnegie Mellon University, Pittsburgh, USA
B. Akgun, R. Carroll, T. Ferguson, Y. Iiyama, D.W. Jang, S.Y. Jun, Y.F. Liu, M. Paulini, J. Russ, H. Vogel, I. Vorobiev

University of Colorado at Boulder, Boulder, USA
J.P. Cumalat, M.E. Dinardo, B.R. Drell, C.J. Edelmaier, W.T. Ford, A. Gaz, B. Heyburn, E. Luiggi Lopez, U. Nauenberg, J.G. Smith, K. Stenson, K.A. Ulmer, S.R. Wagner, S.L. Zang

Cornell University, Ithaca, USA
L. Agostino, J. Alexander, A. Chatterjee, N. Eggert, L.K. Gibbons, B. Heltsley, W. Hopkins,

A. Khukhunaishvili, B. Kreis, G. Nicolas Kaufman, J.R. Patterson, D. Puigh, A. Ryd, E. Salvati, X. Shi, W. Sun, W.D. Teo, J. Thom, J. Thompson, J. Vaughan, Y. Weng, L. Winstrom, P. Wittich

Fairfield University, Fairfield, USA
A. Biselli, G. Cirino, D. Winn

Fermi National Accelerator Laboratory, Batavia, USA
S. Abdullin, M. Albrow, J. Anderson, G. Apollinari, M. Atac, J.A. Bakken, L.A.T. Bauerdick, A. Beretvas, J. Berryhill, P.C. Bhat, I. Bloch, K. Burkett, J.N. Butler, V. Chetluru, H.W.K. Cheung, F. Chlebana, S. Cihangir, W. Cooper, D.P. Eartly, V.D. Elvira, S. Esen, I. Fisk, J. Freeman, Y. Gao, E. Gottschalk, D. Green, O. Gutsche, J. Hanlon, R.M. Harris, J. Hirschauer, B. Hooberman, H. Jensen, S. Jindariani, M. Johnson, U. Joshi, B. Klima, K. Kousouris, S. Kunori, S. Kwan, C. Leonidopoulos, D. Lincoln, R. Lipton, J. Lykken, K. Maeshima, J.M. Marraffino, D. Mason, P. McBride, T. Miao, K. Mishra, S. Mrenna, Y. Musienko[47], C. Newman-Holmes, V. O'Dell, J. Pivarski, R. Pordes, O. Prokofyev, T. Schwarz, E. Sexton-Kennedy, S. Sharma, W.J. Spalding, L. Spiegel, P. Tan, L. Taylor, S. Tkaczyk, L. Uplegger, E.W. Vaandering, R. Vidal, J. Whitmore, W. Wu, F. Yang, F. Yumiceva, J.C. Yun

University of Florida, Gainesville, USA
D. Acosta, P. Avery, D. Bourilkov, M. Chen, S. Das, M. De Gruttola, G.P. Di Giovanni, D. Dobur, A. Drozdetskiy, R.D. Field, M. Fisher, Y. Fu, I.K. Furic, J. Gartner, S. Goldberg, J. Hugon, B. Kim, J. Konigsberg, A. Korytov, A. Kropivnitskaya, T. Kypreos, J.F. Low, K. Matchev, G. Mitselmakher, L. Muniz, P. Myeonghun, R. Remington, A. Rinkevicius, M. Schmitt, B. Scurlock, P. Sellers, N. Skhirtladze, M. Snowball, D. Wang, J. Yelton, M. Zakaria

Florida International University, Miami, USA
V. Gaultney, L.M. Lebolo, S. Linn, P. Markowitz, G. Martinez, J.L. Rodriguez

Florida State University, Tallahassee, USA
T. Adams, A. Askew, J. Bochenek, J. Chen, B. Diamond, S.V. Gleyzer, J. Haas, S. Hagopian, V. Hagopian, M. Jenkins, K.F. Johnson, H. Prosper, S. Sekmen, V. Veeraraghavan

Florida Institute of Technology, Melbourne, USA
M.M. Baarmand, B. Dorney, M. Hohlmann, H. Kalakhety, I. Vodopiyanov

University of Illinois at Chicago (UIC), Chicago, USA
M.R. Adams, I.M. Anghel, L. Apanasevich, Y. Bai, V.E. Bazterra, R.R. Betts, J. Callner, R. Cavanaugh, C. Dragoiu, L. Gauthier, C.E. Gerber, D.J. Hofman, S. Khalatyan, G.J. Kunde[48], F. Lacroix, M. Malek, C. O'Brien, C. Silkworth, C. Silvestre, D. Strom, N. Varelas

The University of Iowa, Iowa City, USA
U. Akgun, E.A. Albayrak, B. Bilki, W. Clarida, F. Duru, C.K. Lae, E. McCliment, J.-P. Merlo, H. Mermerkaya[49], A. Mestvirishvili, A. Moeller, J. Nachtman, C.R. Newsom, E. Norbeck, J. Olson, Y. Onel, F. Ozok, S. Sen, J. Wetzel, T. Yetkin, K. Yi

Johns Hopkins University, Baltimore, USA
B.A. Barnett, B. Blumenfeld, S. Bolognesi, A. Bonato, C. Eskew, D. Fehling, G. Giurgiu, A.V. Gritsan, Z.J. Guo, G. Hu, P. Maksimovic, S. Rappoccio, M. Swartz, N.V. Tran, A. Whitbeck

The University of Kansas, Lawrence, USA
P. Baringer, A. Bean, G. Benelli, O. Grachov, R.P. Kenny Iii, M. Murray, D. Noonan, S. Sanders, R. Stringer, J.S. Wood, V. Zhukova

Kansas State University, Manhattan, USA
A.F. Barfuss, T. Bolton, I. Chakaberia, A. Ivanov, S. Khalil, M. Makouski, Y. Maravin, S. Shrestha, I. Svintradze

Lawrence Livermore National Laboratory, Livermore, USA
J. Gronberg, D. Lange, D. Wright

University of Maryland, College Park, USA
A. Baden, S.C. Eno, J.A. Gomez, N.J. Hadley, R.G. Kellogg, M. Kirn, Y. Lu, A.C. Mignerey, K. Rossato, P. Rumerio, A. Skuja, J. Temple, M.B. Tonjes, S.C. Tonwar, E. Twedt

Massachusetts Institute of Technology, Cambridge, USA
B. Alver, G. Bauer, J. Bendavid, W. Busza, E. Butz, I.A. Cali, M. Chan, V. Dutta, G. Gomez Ceballos, M. Goncharov, K.A. Hahn, P. Harris, Y. Kim, M. Klute, Y.-J. Lee, W. Li, P.D. Luckey, T. Ma, S. Nahn, C. Paus, D. Ralph, C. Roland, G. Roland, M. Rudolph, G.S.F. Stephans, F. Stöckli, K. Sumorok, K. Sung, D. Velicanu, E.A. Wenger, R. Wolf, B. Wyslouch, S. Xie, M. Yang, Y. Yilmaz, A.S. Yoon, M. Zanetti

University of Minnesota, Minneapolis, USA
S.I. Cooper, P. Cushman, B. Dahmes, A. De Benedetti, G. Franzoni, A. Gude, J. Haupt, K. Klapoetke, Y. Kubota, J. Mans, N. Pastika, V. Rekovic, R. Rusack, M. Sasseville, A. Singovsky, J. Turkewitz

University of Mississippi, University, USA
L.M. Cremaldi, R. Godang, R. Kroeger, L. Perera, R. Rahmat, D.A. Sanders, D. Summers

University of Nebraska-Lincoln, Lincoln, USA
E. Avdeeva, K. Bloom, S. Bose, J. Butt, D.R. Claes, A. Dominguez, M. Eads, P. Jindal, J. Keller, I. Kravchenko, J. Lazo-Flores, H. Malbouisson, S. Malik, G.R. Snow

State University of New York at Buffalo, Buffalo, USA
U. Baur, A. Godshalk, I. Iashvili, S. Jain, A. Kharchilava, A. Kumar, K. Smith, Z. Wan

Northeastern University, Boston, USA
G. Alverson, E. Barberis, D. Baumgartel, M. Chasco, S. Reucroft, D. Trocino, D. Wood, J. Zhang

Northwestern University, Evanston, USA
A. Anastassov, A. Kubik, N. Mucia, N. Odell, R.A. Ofierzynski, B. Pollack, A. Pozdnyakov, M. Schmitt, S. Stoynev, M. Velasco, S. Won

University of Notre Dame, Notre Dame, USA
L. Antonelli, D. Berry, A. Brinkerhoff, M. Hildreth, C. Jessop, D.J. Karmgard, J. Kolb, T. Kolberg, K. Lannon, W. Luo, S. Lynch, N. Marinelli, D.M. Morse, T. Pearson, R. Ruchti, J. Slaunwhite, N. Valls, M. Wayne, J. Ziegler

The Ohio State University, Columbus, USA
B. Bylsma, L.S. Durkin, C. Hill, P. Killewald, K. Kotov, T.Y. Ling, M. Rodenburg, C. Vuosalo, G. Williams

Princeton University, Princeton, USA
N. Adam, E. Berry, P. Elmer, D. Gerbaudo, V. Halyo, P. Hebda, A. Hunt, E. Laird, D. Lopes Pegna, P. Lujan, D. Marlow, T. Medvedeva, M. Mooney, J. Olsen, P. Piroué, X. Quan, A. Raval, H. Saka, D. Stickland, C. Tully, J.S. Werner, A. Zuranski

University of Puerto Rico, Mayaguez, USA
J.G. Acosta, X.T. Huang, A. Lopez, H. Mendez, S. Oliveros, J.E. Ramirez Vargas, A. Zatserklyaniy

Purdue University, West Lafayette, USA
E. Alagoz, V.E. Barnes, D. Benedetti, G. Bolla, L. Borrello, D. Bortoletto, M. De Mattia, A. Everett, L. Gutay, Z. Hu, M. Jones, O. Koybasi, M. Kress, A.T. Laasanen, N. Leonardo, V. Maroussov, P. Merkel, D.H. Miller, N. Neumeister, I. Shipsey, D. Silvers, A. Svyatkovskiy, M. Vidal Marono, H.D. Yoo, J. Zablocki, Y. Zheng

Purdue University Calumet, Hammond, USA
S. Guragain, N. Parashar

Rice University, Houston, USA
A. Adair, C. Boulahouache, K.M. Ecklund, F.J.M. Geurts, B.P. Padley, R. Redjimi, J. Roberts, J. Zabel

University of Rochester, Rochester, USA
B. Betchart, A. Bodek, Y.S. Chung, R. Covarelli, P. de Barbaro, R. Demina, Y. Eshaq, H. Flacher, A. Garcia-Bellido, P. Goldenzweig, Y. Gotra, J. Han, A. Harel, D.C. Miner, G. Petrillo, W. Sakumoto, D. Vishnevskiy, M. Zielinski

The Rockefeller University, New York, USA
A. Bhatti, R. Ciesielski, L. Demortier, K. Goulianos, G. Lungu, S. Malik, C. Mesropian

Rutgers, the State University of New Jersey, Piscataway, USA
S. Arora, O. Atramentov, A. Barker, J.P. Chou, C. Contreras-Campana, E. Contreras-Campana, D. Duggan, D. Ferencek, Y. Gershtein, R. Gray, E. Halkiadakis, D. Hidas, D. Hits, A. Lath, S. Panwalkar, M. Park, R. Patel, A. Richards, K. Rose, S. Salur, S. Schnetzer, S. Somalwar, R. Stone, S. Thomas

University of Tennessee, Knoxville, USA
G. Cerizza, M. Hollingsworth, S. Spanier, Z.C. Yang, A. York

Texas A&M University, College Station, USA
R. Eusebi, W. Flanagan, J. Gilmore, A. Gurrola, T. Kamon[50], V. Khotilovich, R. Montalvo, I. Osipenkov, Y. Pakhotin, A. Perloff, J. Roe, A. Safonov, S. Sengupta, I. Suarez, A. Tatarinov, D. Toback

Texas Tech University, Lubbock, USA
N. Akchurin, C. Bardak, J. Damgov, P.R. Dudero, C. Jeong, K. Kovitanggoon, S.W. Lee, T. Libeiro, P. Mane, Y. Roh, A. Sill, I. Volobouev, R. Wigmans, E. Yazgan

Vanderbilt University, Nashville, USA
E. Appelt, E. Brownson, D. Engh, C. Florez, W. Gabella, M. Issah, W. Johns, C. Johnston, P. Kurt, C. Maguire, A. Melo, P. Sheldon, B. Snook, S. Tuo, J. Velkovska

University of Virginia, Charlottesville, USA
M.W. Arenton, M. Balazs, S. Boutle, B. Cox, B. Francis, S. Goadhouse, J. Goodell, R. Hirosky, A. Ledovskoy, C. Lin, C. Neu, J. Wood, R. Yohay

Wayne State University, Detroit, USA
S. Gollapinni, R. Harr, P.E. Karchin, C. Kottachchi Kankanamge Don, P. Lamichhane, M. Mattson, C. Milstène, A. Sakharov

University of Wisconsin, Madison, USA
M. Anderson, M. Bachtis, D. Belknap, J.N. Bellinger, D. Carlsmith, M. Cepeda, S. Dasu, J. Efron, E. Friis, L. Gray, K.S. Grogg, M. Grothe, R. Hall-Wilton, M. Herndon, A. Hervé, P. Klabbers, J. Klukas, A. Lanaro, C. Lazaridis, J. Leonard, R. Loveless, A. Mohapatra, I. Ojalvo, W. Parker, G.A. Pierro, I. Ross, A. Savin, W.H. Smith, J. Swanson, M. Weinberg

†: Deceased
1: Also at CERN, European Organization for Nuclear Research, Geneva, Switzerland
2: Also at National Institute of Chemical Physics and Biophysics, Tallinn, Estonia
3: Also at Universidade Federal do ABC, Santo Andre, Brazil
4: Also at California Institute of Technology, Pasadena, USA
5: Also at Laboratoire Leprince-Ringuet, Ecole Polytechnique, IN2P3-CNRS, Palaiseau, France
6: Also at Suez Canal University, Suez, Egypt
7: Also at Cairo University, Cairo, Egypt
8: Also at British University, Cairo, Egypt
9: Also at Fayoum University, El-Fayoum, Egypt
10: Also at Ain Shams University, Cairo, Egypt
11: Also at Soltan Institute for Nuclear Studies, Warsaw, Poland
12: Also at Université de Haute-Alsace, Mulhouse, France
13: Also at Moscow State University, Moscow, Russia
14: Also at Brandenburg University of Technology, Cottbus, Germany
15: Also at Institute of Nuclear Research ATOMKI, Debrecen, Hungary
16: Also at Eötvös Loránd University, Budapest, Hungary
17: Also at Tata Institute of Fundamental Research - HECR, Mumbai, India
18: Also at University of Visva-Bharati, Santiniketan, India
19: Also at Sharif University of Technology, Tehran, Iran
20: Also at Isfahan University of Technology, Isfahan, Iran
21: Also at Shiraz University, Shiraz, Iran
22: Also at Facoltà Ingegneria Università di Roma, Roma, Italy
23: Also at Università della Basilicata, Potenza, Italy
24: Also at Laboratori Nazionali di Legnaro dell' INFN, Legnaro, Italy
25: Also at Università degli studi di Siena, Siena, Italy
26: Also at Faculty of Physics of University of Belgrade, Belgrade, Serbia
27: Also at University of California, Los Angeles, Los Angeles, USA
28: Also at University of Florida, Gainesville, USA
29: Also at Scuola Normale e Sezione dell' INFN, Pisa, Italy
30: Also at INFN Sezione di Roma; Università di Roma "La Sapienza", Roma, Italy
31: Also at University of Athens, Athens, Greece
32: Now at Rutherford Appleton Laboratory, Didcot, United Kingdom
33: Also at The University of Kansas, Lawrence, USA
34: Also at Paul Scherrer Institut, Villigen, Switzerland
35: Also at University of Belgrade, Faculty of Physics and Vinca Institute of Nuclear Sciences, Belgrade, Serbia
36: Also at Institute for Theoretical and Experimental Physics, Moscow, Russia
37: Also at Gaziosmanpasa University, Tokat, Turkey
38: Also at Adiyaman University, Adiyaman, Turkey
39: Also at The University of Iowa, Iowa City, USA
40: Also at Mersin University, Mersin, Turkey
41: Also at Kafkas University, Kars, Turkey
42: Also at Suleyman Demirel University, Isparta, Turkey

43: Also at Ege University, Izmir, Turkey
44: Also at School of Physics and Astronomy, University of Southampton, Southampton, United Kingdom
45: Also at INFN Sezione di Perugia; Università di Perugia, Perugia, Italy
46: Also at Utah Valley University, Orem, USA
47: Also at Institute for Nuclear Research, Moscow, Russia
48: Also at Los Alamos National Laboratory, Los Alamos, USA
49: Also at Erzincan University, Erzincan, Turkey
50: Also at Kyungpook National University, Daegu, Korea